

BFKL Pomeron, Reggeized gluons, and Bern-Dixon-Smirnov amplitudes

 J. Bartels,¹ L. N. Lipatov,^{1,2} and A. Sabio Vera³
¹*II. Institut Theoretical Physics, Hamburg University, Germany*
²*St. Petersburg Nuclear Physics Institute, Russia*
³*CERN, Geneva, Switzerland*

(Received 28 March 2008; published 5 August 2009)

After a brief review of the Balitsky-Fadin-Kuraev-Lipatov (BFKL) approach to Regge processes in QCD and in supersymmetric gauge theories we propose a strategy for calculating the next-to-next-to-leading order corrections to the BFKL kernel. They can be obtained in terms of various cross sections for Reggeized gluon interactions. The corresponding amplitudes can be calculated in the framework of the effective action for high-energy scattering. In the case of $N = 4$ supersymmetry it is also possible to use the Bern-Dixon-Smirnov ansatz. For this purpose the analytic properties of the Bern-Dixon-Smirnov amplitudes at high energies are investigated, in order to verify their self-consistency. It is found that, for the number of external particles being larger than 5, these amplitudes, beyond one loop, are not in agreement with the BFKL approach which predicts the existence of Regge cuts in some physical channels.

DOI: 10.1103/PhysRevD.80.045002

PACS numbers: 11.15.Bt

I. INTRODUCTION

The elastic scattering amplitude in QCD at high energies for particles with color indices A, B and helicities λ_A, λ_B in the leading logarithmic approximation (LLA) has the Regge form [1]

$$A_{2 \rightarrow 2} = 2g \delta_{\lambda_A \lambda_{A'}} T_{AA'}^c \frac{s^{1+\omega(t)}}{t} g T_{BB'}^c \delta_{\lambda_B \lambda_{B'}}, \quad t = -\vec{q}^2. \quad (1)$$

The gluon Regge trajectory, $j(t) = 1 + \omega(t)$, reads

$$\begin{aligned} \omega(-\vec{q}^2) &= -\frac{\alpha_s N_c}{(2\pi)^2} (2\pi\mu)^{2\epsilon} \int d^{2-2\epsilon} k \frac{\vec{q}^2}{\vec{k}^2 (\vec{q} - k)^2} \\ &\approx -a \left(\ln \frac{\vec{q}^2}{\mu^2} - \frac{1}{\epsilon} \right), \end{aligned} \quad (2)$$

where we have introduced dimensional regularization with $D = 4 - 2\epsilon$ and the renormalization point μ for the 't Hooft coupling constant

$$a = \frac{\alpha_s N_c}{2\pi} (4\pi e^{-\gamma})^\epsilon. \quad (3)$$

The gluon trajectory is also known in the next-to-leading approximation in QCD [2] and in supersymmetry (SUSY) gauge models [3].

In LLA gluons are produced in the multi-Regge kinematics (see Fig. 1). In this kinematics the gluon production amplitude in LLA has the factorized form

$$\begin{aligned} A_{2 \rightarrow 2+n} &= -2sg \delta_{\lambda_A \lambda_{A'}} T_{AA'}^c \frac{s_1^{\omega(-\vec{q}_1^2)}}{\vec{q}_1^2} g C_\mu(q_2, q_1) e_\mu^*(k_1) T_{c_2 c_1}^{d_1} \\ &\times \frac{s_2^{\omega(-\vec{q}_2^2)}}{\vec{q}_2^2} \dots \frac{s_{n+1}^{\omega(-\vec{q}_{n+1}^2)}}{\vec{q}_{n+1}^2} g \delta_{\lambda_B \lambda_{B'}} T_{BB'}^{c_{n+1}}, \end{aligned} \quad (4)$$

where

$$s = (p_A + p_B)^2 \gg s_r = (k_r + k_{r-1})^2 \gg \vec{q}_r^2, \quad (5)$$

$$k_r = q_{r+1} - q_r.$$

The matrices T_{bc}^a are the generators of the $SU(N_c)$ gauge group in the adjoint representation and $C_\mu(q_2, q_1)$ are the effective Reggeon-Reggeon-gluon vertices. In the case when the polarization vector $e_\mu(k_1)$ corresponds to a produced gluon with a definite helicity one can obtain [4]

$$C \equiv C_\mu(q_2, q_1) e_\mu^*(k_1) = \sqrt{2} \frac{q_2^* q_1}{k_1^*}, \quad (6)$$

where the complex notation $q = q_x + iq_y$ for the two-dimensional transverse vectors has been used.

The elastic scattering amplitude with the vacuum quantum numbers in the t -channel can be calculated with the use of s -channel unitarity [1]. In this approach the Pomeron appears as a composite state of two Reggeized gluons. It is also convenient to use transverse coordinates in a complex

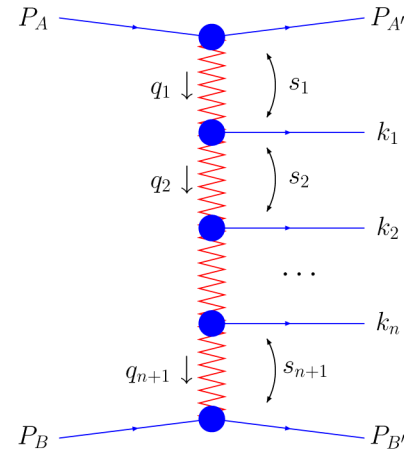


FIG. 1 (color online). Multi-Regge kinematics.

form together with their canonically conjugated momenta as

$$\begin{aligned} \rho_k &= x_k + iy_k, & \rho_k^* &= x_k - iy_k, \\ p_k &= i \frac{\partial}{\partial \rho_k}, & p_k^* &= i \frac{\partial}{\partial \rho_k^*}. \end{aligned} \quad (7)$$

In the coordinate representation the Balitsky-Fadin-Kuraev-Lipatov (BFKL) equation for the Pomeron wave function can then be written as follows [1]:

$$E\Psi(\vec{\rho}_1, \vec{\rho}_2) = H_{12}\Psi(\vec{\rho}_1, \vec{\rho}_2), \quad \Delta = -\frac{\alpha_s N_c}{2\pi} \min E, \quad (8)$$

where Δ is the Pomeron intercept. The BFKL Hamiltonian has the rather simple representation [5]

$$\begin{aligned} H_{12} &= \ln|p_1 p_2|^2 + \frac{1}{p_1 p_2^*} (\ln|\rho_{12}|^2) p_1 p_2^* \\ &+ \frac{1}{p_1^* p_2} (\ln|\rho_{12}|^2) p_1^* p_2 - 4\psi(1), \end{aligned} \quad (9)$$

with $\rho_{12} = \rho_1 - \rho_2$. The kinetic energy is proportional to the sum of two gluon Regge trajectories $\omega(-|p_i|^2)$ ($i = 1, 2$). The potential energy $\sim \ln|\rho_{12}|^2$ is related to the product of two gluon production vertices C_μ . This Hamiltonian is invariant under the Möbius transformation [6]

$$\rho_k \rightarrow \frac{a\rho_k + b}{c\rho_k + d}, \quad (10)$$

where a, b, c and d are complex numbers. The eigenvalues of the corresponding Casimir operators are expressed in terms of the conformal weights

$$m = \frac{1}{2} + i\nu + \frac{n}{2}, \quad \tilde{m} = \frac{1}{2} + i\nu - \frac{n}{2} \quad (11)$$

for the unitary principal series representation of $SL(2, C)$, with ν being real and n integer.

The BFKL Hamiltonian can be iterated in the s -channel to account for the exchange of an arbitrary number of Reggeized gluons. This iteration is described by the Bartels-Kwiecinski-Praszalowicz (BKP) equation [7] for the n -gluon colorless composite state. In the $N_c \rightarrow \infty$ limit the Hamiltonian has the property of holomorphic separability [8] in the form

$$H = \frac{1}{2} \sum_k H_{k,k+1} = \frac{1}{2} (h + h^*), \quad [h, h^*] = 0. \quad (12)$$

The holomorphic Hamiltonian can be written as

$$h = \sum_k h_{k,k+1}, \quad (13)$$

$$h_{12} = \ln(p_1 p_2) + \frac{1}{p_1} (\ln\rho_{12}) p_1 + \frac{1}{p_2} (\ln\rho_{12}) p_2 - 2\psi(1),$$

where $\psi(x) = (\ln\Gamma(x))'$. Consequently, the wave function

Ψ fulfills holomorphic factorization [8] and there exists the remarkable duality symmetry under the transformation [9]

$$p_i \rightarrow p_{i,i+1} \rightarrow p_{i+1}. \quad (14)$$

Moreover, in the holomorphic and antiholomorphic sectors, there are integrals of motion commuting among themselves and with h [5,10]:

$$q_r = \sum_{k_1 < k_2 < \dots < k_r} \rho_{k_1 k_2} \rho_{k_2 k_3} \dots \rho_{k_{r-1} k_r} p_{k_1} p_{k_2} \dots p_{k_r}, \quad (15)$$

$$[q_r, h] = 0.$$

The integrability of BFKL dynamics was demonstrated in [10], and it is related to the fact that h coincides with the local Hamiltonian of the Heisenberg spin model [11]. In the LLA the Pomeron intercept is $\Delta = 4 \frac{\alpha_s}{\pi} N_c \ln 2 > 0$ and the Froissart bound $\sigma_t < c \ln^2 s$ for the total cross section $\sigma_t \sim s^\Delta$ is violated [1].

In the next-to-leading logarithmic approximation the integral kernel for the BFKL equation was constructed in Refs. [3,12]. Because of its Möbius invariance, the solution of the BFKL equation can be classified by the anomalous dimension $\gamma = \frac{1}{2} + i\nu$ of twist-2 operators and the conformal spin $|n|$, which coincides with the number of transverse indices of the local operators $O_{\mu_1 \dots \mu_j}$.

The eigenvalue of the BFKL kernel in the next-to-leading approximation has the form [12]

$$\begin{aligned} \omega &= 4\hat{a} \left[2\psi(1) - \psi\left(\gamma + \frac{|n|}{2}\right) - \psi\left(1 - \gamma + \frac{|n|}{2}\right) \right] \\ &+ 4\hat{a}^2 \Delta(n, \gamma), \\ \hat{a} &= g^2 \frac{N_c}{16\pi^2}. \end{aligned} \quad (16)$$

In QCD, the next-to-leading contribution $\Delta(n, \gamma)$ is a non-analytic function of the conformal spin $|n|$ because it contains some terms depending on the Kronecker symbols $\delta_{n,0}$ and $\delta_{n,2}$. However, in $N = 4$ SUSY this dependence is cancelled and we obtain the following hermitially separable expression [3,13]:

$$\Delta(n, \gamma) = \phi(M) + \phi(M^*) - \frac{\rho(M) + \rho(M^*)}{2\hat{a}/\omega}, \quad (17)$$

$$M = \gamma + \frac{|n|}{2},$$

$$\rho(M) = \beta'(M) + \frac{1}{2} \zeta(2), \quad (18)$$

$$\beta'(z) = \frac{1}{4} \left[\Psi'\left(\frac{z+1}{2}\right) - \Psi'\left(\frac{z}{2}\right) \right],$$

where

$$\begin{aligned} \phi(M) &= 3\zeta(3) + \psi''(M) - 2\Phi(M) \\ &+ 2\beta'(M)(\psi(1) - \psi(M)), \end{aligned} \quad (19)$$

and

$$\Phi(M) = \sum_{k=0}^{\infty} \frac{\beta'(k+1)}{k+M} + \sum_{k=0}^{\infty} \frac{(-1)^k}{k+M} \times \left(\psi'(k+1) - \frac{\psi(k+1) - \psi(1)}{k+M} \right). \quad (20)$$

Very importantly, all these contributions have the property of maximal transcendentality [13]. The behavior of the 4-point Green function corresponding to this NLO kernel in $N = 4$ SUSY was investigated in [14]. The NLO conformal spins affect azimuthal angle decorrelations in jet physics as it was originally suggested in [15].

In a different context, the one-loop anomalous dimension matrix for twist-2 operators in $N = 4$ SUSY can be easily calculated since it is completely fixed by superconformal invariance. Its eigenvalue is proportional to $\psi(1) - \psi(j-1)$, which is related to the integrability of the evolution equation for the quasiparton operators in this model [16]. The integrability of $N = 4$ SUSY has also been established for other operators and in higher loops [17,18].

The maximal transcendentality principle suggested in Ref. [13] made it possible to extract the universal anomalous dimension up to three loops in $N = 4$ SUSY [19,20] from the QCD results [21]. This principle was also helpful for finding closed integral equations for the cusp anomalous dimension in this model [22,23] based on the AdS/CFT correspondence [24–26]. In the framework of the asymptotic Bethe ansatz the maximal transcendentality principle helped to fix the anomalous dimension at four loops [27]. However, the obtained results contradict the predictions stemming from the BFKL equation [3,13]. The origin of this discrepancy is related to the onset of wrapping effects [27]. In this framework it is, therefore, crucial to obtain more information from the BFKL side through the calculation of its higher order corrections to the integral kernel. We would like to point out that the intercept of the BFKL Pomeron at large 't Hooft coupling constant in $N = 4$ SUSY was found in Refs. [20,28].

In the present article we want to formulate a program to calculate the three-loop corrections to the BFKL kernel in the 't Hooft coupling. Our approach is based on the use of the high-energy effective action developed in [29,30] for the construction of the various Reggeized gluon couplings, and on the BDS ansatz [31] for scattering amplitudes in the $N = 4$ super Yang-Mills theory. We begin with a short review of the effective action (Sec. II) and then turn to an analysis of the BDS formula in the Regge limit for the amplitudes up to six external gluons (Sec. III). An interpretation based upon known results of the high-energy limit of scattering amplitudes in QCD is given in Sec. IV. An outlook is presented in the concluding section. Some details of the calculations are presented in several appendices.

II. EFFECTIVE ACTION FOR REGGEIZED GLUONS

Initially calculations of scattering amplitudes in Regge kinematics were performed by an iterative method based on analyticity, unitarity and renormalizability of the theory [1]. The s -channel unitarity was incorporated partly in the form of bootstrap equations for the amplitudes generated by Reggeized gluons exchange. But later it turned out that for this purpose one can also use an effective field theory for Reggeized gluons [29,30].

We shall write below the effective action valid at high energies for interactions of particles inside each cluster having their rapidities y in a certain interval

$$y = \frac{1}{2} \ln \frac{\epsilon_k + |k|}{\epsilon_k - |k|}, \quad |y - y_0| < \eta, \quad \eta \ll \ln s. \quad (21)$$

The corresponding gluon and quark fields are

$$v_\mu(x) = -iT^a v_\mu^a(x), \quad \psi(x), \quad \bar{\psi}(x), \quad [T^a, T^b] = if_{abc} T^c. \quad (22)$$

In the case of the supersymmetric models one can take into account also the fermion and scalar fields with known Yang-Mills and Yukawa interactions. Let us introduce now the fields describing the production and annihilation of Reggeized gluons [29]:

$$A_\pm(x) = -iT^a A_\pm^a(x). \quad (23)$$

Under the global color group rotations the fields are transformed in the standard way

$$\begin{aligned} \delta v_\mu(x) &= [v_\mu(x), \chi], & \delta \psi(x) &= -\chi \psi(x), \\ \delta A(x) &= [A(x), \chi], \end{aligned} \quad (24)$$

but under the local gauge transformations with $\chi(x) \rightarrow 0$ at $x \rightarrow \infty$ we have

$$\begin{aligned} \delta v_\mu(x) &= \frac{1}{g} [D_\mu, \chi(x)], & \delta \psi(x) &= -\chi(x) \psi(x), \\ \delta A_\pm(x) &= 0. \end{aligned} \quad (25)$$

In quasi-multi-Regge kinematics particles are produced in groups (clusters) with fixed masses. These groups have significantly different rapidities corresponding to the multi-Regge asymptotics. In this case one obtains the following kinematical constraint on the Reggeon fields

$$\partial_\mp A_\pm(x) = 0, \quad \partial_\pm = n_\pm^\mu \partial_\mu, \quad (26)$$

$n_\pm^\mu = \delta_0^\mu \pm \delta_3^\mu$. For QCD the corresponding effective action local in the rapidity y has the form [29]

$$S = \int d^4x (L_0 + L_{\text{ind}}), \quad (27)$$

where L_0 is the usual Yang-Mills Lagrangian

$$L_0 = i\bar{\psi} \hat{D} \psi + \frac{1}{2} \text{Tr} G_{\mu\nu}^2, \quad D_\mu = \partial_\mu + g v_\mu, \quad (28)$$

$$G_{\mu\nu} = \frac{1}{g} [D_\mu, D_\nu]$$

and the induced contribution is given by

$$L_{\text{ind}} = \text{Tr}(L_{\text{ind}}^k + L_{\text{ind}}^{GR}), \quad L_{\text{ind}}^k = -\partial_\mu A_+^a \partial_\mu A_-^a. \quad (29)$$

Here the Reggeon-gluon interaction can be presented in terms of Wilson P -exponents

$$L_{\text{ind}}^{GR} = -\frac{1}{g} \partial_+ P \exp\left(-g \frac{1}{2} \int_{-\infty}^{x^+} v_+(x') d(x')^+\right) \partial_\sigma^2 A_-$$

$$- \frac{1}{g} \partial_- P \exp\left(-g \frac{1}{2} \int_{-\infty}^{x^-} v_-(x') d(x')^+\right) \partial_\sigma^2 A_+$$

$$= \left(v_+ - g v_+ \frac{1}{\partial_+} v_+ + g^2 v_+ \frac{1}{\partial_+} v_+ \frac{1}{\partial_+} v_+ - \dots\right)$$

$$\times \partial_\sigma^2 A_- + \left(v_- - g v_- \frac{1}{\partial_-} v_- + g^2 v_- \frac{1}{\partial_-} v_- \frac{1}{\partial_-} v_- - \dots\right) \partial_\sigma^2 A_+. \quad (30)$$

One can formulate the Feynman rules directly in momentum space [30]. For this purpose it is needed to take into account the gluon momentum conservation for induced vertices

$$k_0^\pm + k_1^\pm + \dots + k_r^\pm = 0. \quad (31)$$

Some simple examples of induced Reggeon-gluon vertices are

$$\Delta_{a_0 c}^{\nu_0 +} = \tilde{q}_\perp^2 \delta_{a_0 c} (n^+)^{\nu_0}, \quad (32)$$

$$\Delta_{a_0 a_1 c}^{\nu_0 \nu_1 +} = \tilde{q}_\perp^2 T_{a_1 a_0}^c (n^+)^{\nu_1} \frac{1}{k_1^+} (n^+)^{\nu_0},$$

$$\Delta_{a_0 a_1 a_2 c}^{\nu_0 \nu_1 \nu_2 +} = \tilde{q}_\perp^2 (n^+)^{\nu_0} (n^+)^{\nu_1} (n^+)^{\nu_2} \left(\frac{T_{a_2 a_0}^a T_{a_1 a}^c}{k_1^+ k_2^+} + \frac{T_{a_2 a_1}^a T_{a_0 a}^c}{k_0^+ k_2^+} \right). \quad (33)$$

In the general case these vertices factorize in the form

$$\Delta_{a_0 a_1 \dots a_r c}^{\nu_0 \nu_1 \dots \nu_r +} = (-1)^r \tilde{q}_\perp^2 \prod_{s=0}^r (n^+)^{\nu_s} 2 \text{Tr}(T^c G_{a_0 a_1 \dots a_r}), \quad (34)$$

where T^c are the color generators in the fundamental representation. In more detail, $G_{a_0 a_1 \dots a_r}$ can be written as [30]

$$G_{a_0 a_1 \dots a_r} = \sum_{\{i_0, i_1, \dots, i_r\}} \frac{T^{a_{i_0}} T^{a_{i_1}} T^{a_{i_2}} \dots T^{a_{i_r}}}{k_{i_0}^+ (k_{i_0}^+ + k_{i_1}^+) \dots (k_{i_0}^+ + k_{i_1}^+ + \dots + k_{i_{r-1}}^+)}. \quad (35)$$

These vertices satisfy the following recurrent relations (Ward identities) [29]

$$k_r^+ \Delta_{a_0 a_1 \dots a_r c}^{\nu_0 \nu_1 \dots \nu_r +} (k_0^+, \dots, k_r^+)$$

$$= -(n^+)^{\nu_r} \sum_{i=0}^{r-1} i f_{aa_r a_i} \Delta_{a_0 \dots a_{i-1} a_{i+1} \dots a_{r-1} c}^{\nu_0 \dots \nu_{r-1} +}$$

$$\times (k_0^+, \dots, k_{i-1}^+, k_i^+ + k_r^+, k_{i+1}^+, \dots, k_{r-1}^+). \quad (36)$$

With the use of this effective theory one can calculate the tree amplitude for the production of a cluster of three gluons, or a gluon and a pair of fermions or scalar particles (in the case of an extended supersymmetric model) in the collision of two Reggeized gluons [30] (see also earlier calculations of this amplitude in [32]). The square of the amplitude for three particle production integrated over the momenta of these particles is the main ingredient to construct the corresponding contribution to the BFKL kernel in the next-to-next-to-leading approximation using the methods of [33]. One can go to the helicity basis of produced gluons or fermions [34]. In principle it is also possible to calculate the loop corrections to the above Reggeon-particle vertices with the use of the effective action, however, in the present paper, we will use for this purpose the results for $N = 4$ SUSY amplitudes presented by Bern, Dixon and Smirnov in [31].

III. BDS AMPLITUDES IN MULTI-REGGE KINEMATICS

As we have already remarked in the previous section, to find the next-to-next-to-leading corrections to the BFKL kernel in $N = 4$ SUSY we need to calculate, apart from the amplitude for the transition of two Reggeized gluons to three particles, also the three-loop correction to the gluon Regge trajectory, the two-loop correction to the Reggeon-Reggeon-gluon vertex, and the one-loop correction to the amplitude for the transition of two Reggeized gluons to two gluons or their superpartners. In this section we consider, as a first step, the corrections to the Regge trajectory and corrections to the Reggeon-Reggeon-gluon vertex (valid up to one loop) which can be obtained from the multi-Regge asymptotics of the amplitude with the maximal helicity violation, calculated by Bern, Dixon and Smirnov (BDS) [31]. We also investigate the 6-point amplitudes $2 \rightarrow 4$ and $3 \rightarrow 3$ in multi-Regge kinematics, thus preparing the comparison with QCD calculations to be carried out in the following section.

The BDS formula determines the logarithm of the scattering amplitude (to be more precise: after the Born amplitude has been removed). In our analysis of the BDS formula we will, throughout our paper, restrict ourselves, in the logarithm of the amplitudes, to those terms which are singular or constant in ϵ , i.e. we do not (yet) consider corrections of order ϵ or ϵ^2 in the logarithm of the amplitude. As a consequence, all results for the scattering amplitude are correct up to relative corrections of the order ϵ , i.e. all results should be multiplied by a factor of the form

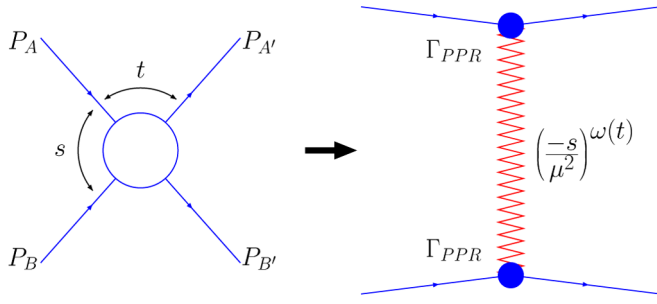


FIG. 2 (color online). Elastic scattering in the Regge asymptotics.

($1 + \mathcal{O}(\epsilon)$). Details of our analysis of the BDS formula are outlined in several appendices.

According to Ref. [31], in the case of maximal helicity violation the amplitude A_n with n legs in the large- N_c limit is factorized in the product of the tree result (including the corresponding color structure) and the simple scalar quantity M_n . In the Regge limit $s \gg (-t)$ the expression for M_4 having the singularities in s and t -channels can be simplified as follows (see Fig. 2 and Appendix A):¹

$$M_{2 \rightarrow 2} = \Gamma(t) \left(\frac{-s}{\mu^2}\right)^{\omega(t)} \Gamma(t) \cdot (1 + \mathcal{O}(\epsilon)), \quad (37)$$

where μ^2 is the renormalization point,

$$\omega(t) = -\frac{\gamma(a)}{4} \ln \frac{-t}{\mu^2} + \int_0^a \frac{da'}{a'} \left(\frac{\gamma(a')}{4\epsilon} + \beta(a') \right), \quad (38)$$

is the all-order gluon Regge trajectory, as obtained from the BDS formula [35,36] (for a verification by comparison with explicit calculations see discussions below), and

$$\begin{aligned} \ln \Gamma(t) = & \ln \frac{-t}{\mu^2} \int_0^a \frac{da'}{a'} \left(\frac{\gamma(a')}{8\epsilon} + \frac{\beta(a')}{2} \right) + \frac{C(a)}{2} + \frac{\gamma(a)}{2} \zeta_2 \\ & - \int_0^a \frac{da'}{a'} \ln \frac{a}{a'} \left(\frac{\gamma(a')}{4\epsilon^2} + \frac{\beta(a')}{\epsilon} + \delta(a') \right), \end{aligned} \quad (39)$$

is the vertex for the coupling of the Reggeized gluon to the external particles.

¹As we have said before, the factor $(1 + \mathcal{O}(\epsilon))$ on the right-hand side is present in all our results for scattering amplitudes, and it will be omitted in the following. For example, for the calculation of the vertex function Γ , from the BDS formula, our neglect of order- ϵ corrections in the logarithm has consequences: in order to determine the vertex function beyond the one-loop approximation, it is necessary to compute, in the logarithm, also the higher order terms. However, such a computation is not the aim of this paper, and we will not go beyond the one-loop approximations for the logarithm of vertex functions, $\ln \Gamma(t)$ or $\ln \Gamma(t_2, t_1, \ln \kappa)$ (see below). We will have to come back to this question when calculating the full higher order corrections to the BFKL equation. We thank V. Del Duca for discussions on this point.

The 't Hooft coupling is defined as in Eq. (3):

$$a = \frac{\alpha N_c}{2\pi} (4\pi e^{-\gamma})^\epsilon \quad (40)$$

and the small parameter ϵ is related to the dimensional regularization $4 \rightarrow 4 - 2\epsilon$. The cusp anomalous dimension $\gamma(a)$ is known to all loops [20,23,37]

$$\gamma(a) = 4a - 4\zeta_2 a^2 + 22\zeta_4 a^3 + \dots, \quad (41)$$

and the functions $\beta(a)$, $\delta(a)$ and $C(a)$ read [31]

$$\begin{aligned} \beta(a) = & -\zeta_3 a^2 + (6\zeta_5 + 5\zeta_2 \zeta_3) a^3 + \dots, \\ \delta(a) = & -\zeta_4 a^2 + \dots, \quad C(a) = -\frac{\zeta_2^2}{2} a^2 + \dots, \end{aligned} \quad (42)$$

where $\zeta(n)$ is the Riemann ζ -function

$$\zeta(n) = \sum_{k=1}^{\infty} k^{-n}. \quad (43)$$

Written as in Eq. (37) we can see that the asymptotic behavior of the $M_{2 \rightarrow 2}$ BDS amplitude corresponds to the Regge ansatz with the gluon trajectory $j = 1 + \omega(t)$ given by the perturbative expansion

$$\begin{aligned} \omega(t) = & \left(-\ln \frac{-t}{\mu^2} + \frac{1}{\epsilon} \right) a + \left[\zeta_2 \left(\ln \frac{-t}{\mu^2} - \frac{1}{2\epsilon} \right) - \frac{\zeta_3}{2} \right] a^2 \\ & + \left[-\frac{11}{2} \zeta_4 \left(\ln \frac{-t}{\mu^2} - \frac{1}{3\epsilon} \right) + \frac{6\zeta_5 + 5\zeta_2 \zeta_3}{3} \right] a^3 + \dots \end{aligned} \quad (44)$$

The first two terms in this expansion are in agreement with the predictions in Refs. [1,3]. Note that in Ref. [3], where the BFKL kernel at NLO was calculated in $N = 4$ SUSY, initially the $\overline{\text{MS}}$ -scheme was used, and only later, in Ref. [13], the final result was also presented in the dimensional reduction scheme (DRED). The NLO terms in the BDS expression for $\omega(t)$ can be obtained from Ref. [3] by converting it to the DRED scheme, where, apart from the finite renormalization of the coupling constant, one should also take into account in the loop the additional number 2ϵ of scalar particles (for details see Appendix A and the recent paper [38]).² The $\mathcal{O}(a^3)$ term in $\omega(t)$, extracted from the BDS amplitude [35]), corresponds to the three-loop correction to the gluon Regge trajectory needed when calculating the next-to-next-to-leading corrections to the BFKL kernel in this model. Strictly speaking the Regge asymptotics of scattering amplitudes corresponds to a different order of taking two limits $\epsilon \rightarrow 0$ and $s \rightarrow \infty$, but it is probable that they can be interchanged.

It is noteworthy to point out that the expression for $M_{2 \rightarrow 2}$, derived in the Regge kinematics, in fact, is valid also outside the Regge limit. That is to say that, when

²We thank A. V. Kotikov and E. M. Levin for helpful discussions regarding these redefinitions.

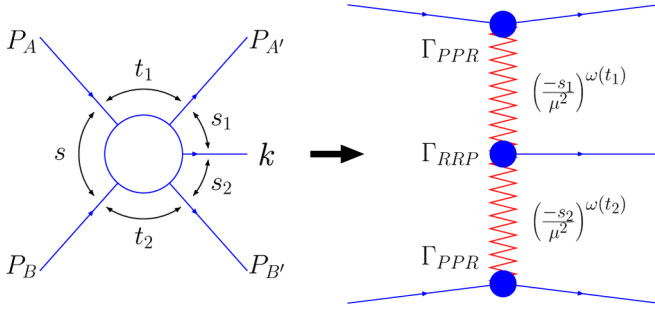


FIG. 3 (color online). Production amplitude in the multi-Regge regime.

analyzing the BDS formula for the logarithm of the $2 \rightarrow 2$ amplitude (see Appendix A), we do not make use of the high-energy limit. In particular, the amplitude can also be written in the dual form

$$M_{2 \rightarrow 2} = \Gamma(s) \left(\frac{-t}{\mu^2} \right)^{\omega(s)} \Gamma(s). \quad (45)$$

After having described the elastic scattering amplitude we now focus on the BDS production amplitude (see Fig. 3). The analysis of $\ln M_{2 \rightarrow 3}$, described in

Appendix B shows that the amplitude (as before, up to the corrections $(1 + \mathcal{O}(\epsilon))$: see also footnote 1) can be written in the factorized form

$$M_{2 \rightarrow 3} = \Gamma(t_1) \left(\frac{-s_1}{\mu^2} \right)^{\omega(t_1)} \Gamma(t_2, t_1, \ln -\kappa) \left(\frac{-s_2}{\mu^2} \right)^{\omega(t_2)} \Gamma(t_2), \quad (46)$$

with

$$-\kappa = \frac{(-s_1)(-s_2)}{(-s)}. \quad (47)$$

Since Eq. (46) is exact it is also valid in the multi-Regge kinematics

$$-s \gg -s_1, \quad -s_2 \gg -t_1 \sim -t_2 \sim -\kappa, \quad (48)$$

where all invariants s, s_1, s_2, t_1 and t_2 are negative. Because of the correct factorization properties of this amplitude the Reggeon-particle-particle vertex $\Gamma(t)$ in Eq. (46) is exactly the same as in the elastic amplitude in Eq. (39). The gluon Regge trajectory $\omega(t)$ in Eq. (46) also coincides with the one discussed above. The new component is the Reggeon-Reggeon-particle vertex. Its logarithm is given by

$$\begin{aligned} \ln \Gamma(t_2, t_1, \ln -\kappa) = & -\frac{\gamma(a)}{16} \ln^2 \frac{-\kappa}{\mu^2} - \frac{1}{2} \int_0^a \frac{da'}{a'} \ln \frac{a}{a'} \left(\frac{\gamma(a')}{4\epsilon^2} + \frac{\beta(a')}{\epsilon} + \delta(a') \right) - \frac{\gamma(a)}{16} \ln^2 \frac{-t_1}{-t_2} - \frac{\gamma(a)}{16} \zeta_2 \\ & - \frac{1}{2} \left(\omega(t_1) + \omega(t_2) - \int_0^a \frac{da'}{a'} \left(\frac{\gamma(a')}{4\epsilon} + \beta(a') \right) \right) \ln \frac{-\kappa}{\mu^2}. \end{aligned} \quad (49)$$

It is now possible to analytically continue this $2 \rightarrow 3$ production amplitude to the physical region where the invariants s, s_1 and s_2 are positive (see Fig. 4(a))

$$\begin{aligned} M_{2 \rightarrow 3} = & \Gamma(t_1) \left(\frac{-s_1 - i\epsilon}{\mu^2} \right)^{\omega(t_1)} \Gamma(t_2, t_1, \ln \kappa - i\pi) \\ & \times \left(\frac{-s_2 - i\epsilon}{\mu^2} \right)^{\omega(t_2)} \Gamma(t_2). \end{aligned} \quad (50)$$

A similar continuation to another physical region can be performed in the case when s is positive but s_1 and s_2 are negative (see Fig. 4(b)):

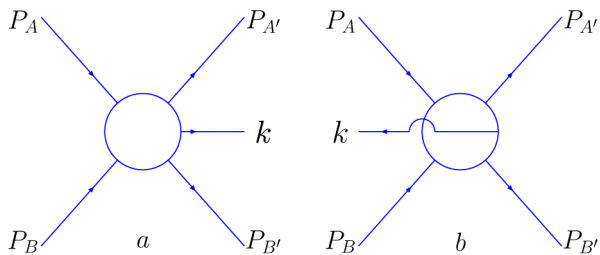


FIG. 4 (color online). Physical channels for the one particle production amplitude.

$$\begin{aligned} M_{2 \rightarrow 3} = & \Gamma(t_1) \left(\frac{-s_1}{\mu^2} \right)^{\omega(t_1)} \Gamma(t_2, t_1, \ln \kappa + i\pi) \\ & \times \left(\frac{-s_2}{\mu^2} \right)^{\omega(t_2)} \Gamma(t_2). \end{aligned} \quad (51)$$

Using a “dispersive” representation illustrated in Fig. 5 (in the following, we will refer to this type of representation as “analytic” representation), it can be easily verified that in all physical regions (including the crossing channels with $s, s_1 < 0, s_2 > 0$ and $s, s_2 < 0, s_1 > 0$) the amplitude can be written as follows:

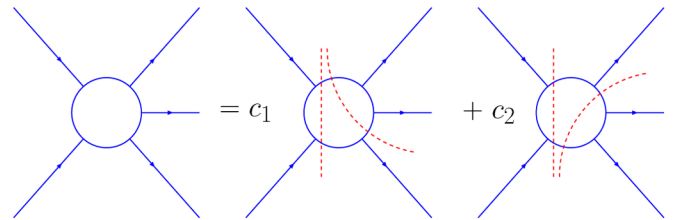


FIG. 5 (color online). Dispersion representation for $M_{2 \rightarrow 3}$, exhibiting its analytic structure.

$$\begin{aligned} \frac{M_{2 \rightarrow 3}}{\Gamma(t_1)\Gamma(t_2)} &= \left(\frac{-s_1}{\mu^2}\right)^{\omega(t_1)-\omega(t_2)} \left(\frac{-s\kappa}{\mu^4}\right)^{\omega(t_2)} c_1 \\ &+ \left(\frac{-s_2}{\mu^2}\right)^{\omega(t_2)-\omega(t_1)} \left(\frac{-s\kappa}{\mu^4}\right)^{\omega(t_1)} c_2 \end{aligned} \quad (52)$$

with the real coefficients c_i

$$c_1 = |\Gamma(t_2, t_1, \ln-\kappa)| \frac{\sin\pi(\omega(t_1) - \phi_\Gamma)}{\sin\pi(\omega(t_1) - \omega(t_2))}, \quad (53)$$

$$c_2 = |\Gamma(t_2, t_1, \ln-\kappa)| \frac{\sin\pi(\omega(t_2) - \phi_\Gamma)}{\sin\pi(\omega(t_2) - \omega(t_1))}, \quad (54)$$

where ϕ_Γ is the phase of Γ , i.e.

$$\Gamma(t_2, t_1, \ln\kappa - i\pi) = |\Gamma(t_2, t_1, \ln-\kappa)| e^{i\pi\phi_\Gamma}. \quad (55)$$

In this dispersion-type representation for all physical channels we use the on-mass shell constraint for the produced gluon momentum

$$\kappa = \vec{k}_\perp^2 = (\vec{q}_1 - \vec{q}_2)^2, \quad (56)$$

where \vec{k}_\perp is its transverse component ($k_\perp p_A = k_\perp p_B = 0$). In this case the amplitude $M_{2 \rightarrow 3}$ does not have simultaneous singularities in the overlapping channels (s_1, s_2), in an agreement with the condition of the gluon stability (this will be discussed further in Sec. IV B).

The fact that there exists a solution for the coefficients c_1 and c_2 proves that the scattering amplitude, derived from the BDS formula, has the correct analytic structure in all physical regions. In particular, it satisfies the Steinmann relations (a somewhat more detailed discussion of analyticity properties will be presented in the following section). We therefore conclude that the BDS amplitude for the production of one particle in multi-Regge kinematics has the correct multi-Regge form. This is encouraging, and we proceed now to study the production of two particles in multi-Regge kinematics, for which we use the $M_{2 \rightarrow 4}$ BDS scattering amplitudes.

We have first checked that the planar BDS amplitude for two particle production having singularities only at positive values of the invariants $s, s_1, s_2, s_3, t_1, t_2, t_3$ has the correct multi-Regge form in the multi-Regge kinematics in the region where all invariants $s, s_1, s_2, s_3, t_1, t_2, t_3$ are negative (see Fig. 6 and Appendix C)

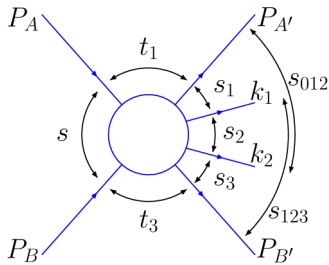


FIG. 6 (color online). Production of two particles.

$$\begin{aligned} \frac{M_{2 \rightarrow 4}}{\Gamma(t_1)\Gamma(t_3)} &= \left(\frac{-s_1}{\mu^2}\right)^{\omega(t_1)} \Gamma(t_2, t_1, \ln-\kappa_{12}) \\ &\times \left(\frac{-s_2}{\mu^2}\right)^{\omega(t_2)} \Gamma(t_3, t_2, \ln-\kappa_{23}) \left(\frac{-s_3}{\mu^2}\right)^{\omega(t_3)} \end{aligned} \quad (57)$$

and the quantities

$$-\kappa_{12} = \frac{(-s_1)(-s_2)}{-s_{012}}, \quad -\kappa_{23} = \frac{(-s_2)(-s_3)}{-s_{123}} \quad (58)$$

are fixed together with t_i . The invariants s_{012} and s_{123} are the squared masses of the corresponding three particles in their center-of-mass system.

In a similar way to what we did in the $2 \rightarrow 3$ case, the BDS $2 \rightarrow 4$ amplitude can be analytically continued to several physical channels, each of them corresponding to different signs of the invariants $s, s_{012}, s_{123}, s_1, s_2, s_3$. To begin with, in the region [see Fig. 7(a)]

$$s, s_{012}, s_{123}, s_1, s_2, s_3 > 0 \quad (59)$$

the amplitude has the form

$$\begin{aligned} \frac{M_{2 \rightarrow 4}}{\Gamma(t_1)\Gamma(t_3)} &= \left(\frac{-s_1}{\mu^2}\right)^{\omega(t_1)} \Gamma(t_2, t_1, \ln\kappa_{12} - i\pi) \\ &\times \left(\frac{-s_2}{\mu^2}\right)^{\omega(t_2)} \Gamma(t_3, t_2, \ln\kappa_{23} - i\pi) \\ &\times \left(\frac{-s_3}{\mu^2}\right)^{\omega(t_3)}, \end{aligned} \quad (60)$$

where we can replace κ_{12} and κ_{23} by their values on the mass shell

$$\kappa_{12} \rightarrow \frac{s_1 s_2}{s_{012}} = \vec{k}_{1\perp}^2, \quad \kappa_{23} \rightarrow \frac{s_2 s_3}{s_{123}} = \vec{k}_{2\perp}^2. \quad (61)$$

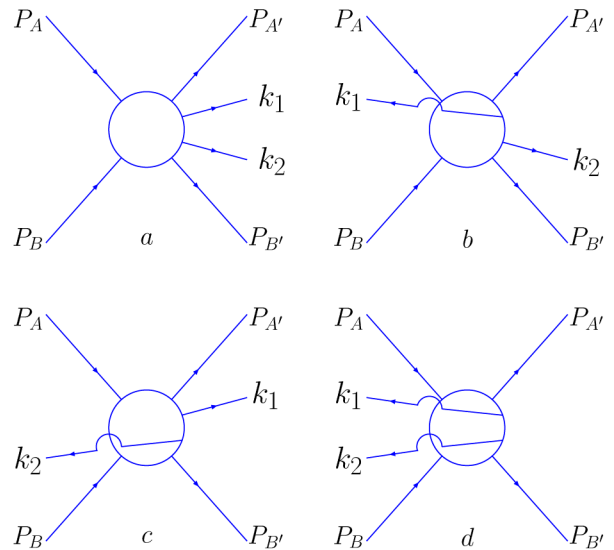


FIG. 7 (color online). Physical channels for two particle production.

Here $k_1 = q_1 - q_2$ and $k_2 = q_2 - q_1$ are the momenta of the produced particles (see Fig. 7).

In the physical region, represented in Fig. 7(b), where

$$s, s_{012}, s_3 > 0, \quad s_1, s_2, s_{123} < 0, \quad (62)$$

one can obtain, for the multi-Regge asymptotics of the BDS amplitude, the following expression:

$$\begin{aligned} \frac{M_{2 \rightarrow 4}}{\Gamma(t_1)\Gamma(t_3)} &= \left(\frac{-s_1}{\mu^2}\right)^{\omega(t_1)} \Gamma(t_2, t_1, \ln \kappa_{12} + i\pi) \\ &\times \left(\frac{-s_2}{\mu^2}\right)^{\omega(t_2)} \Gamma(t_3, t_2, \ln \kappa_{23} - i\pi) \\ &\times \left(\frac{-s_3}{\mu^2}\right)^{\omega(t_3)}. \end{aligned} \quad (63)$$

In a similar way, in the region (see Fig. 7(c))

$$\begin{aligned} \frac{M_{2 \rightarrow 4}}{\Gamma(t_1)\Gamma(t_3)} &= \left(\frac{-s_1}{\mu^2}\right)^{\omega(t_1)-\omega(t_2)} \left(\frac{-s_{012}\kappa_{12}}{\mu^4}\right)^{\omega(t_2)-\omega(t_3)} \left(\frac{-s\kappa_{12}\kappa_{23}}{\mu^6}\right)^{\omega(t_3)} d_1 + \left(\frac{-s_3}{\mu^2}\right)^{\omega(t_3)-\omega(t_2)} \left(\frac{-s_{123}\kappa_{23}}{\mu^4}\right)^{\omega(t_2)-\omega(t_1)} \\ &\times \left(\frac{-s\kappa_{12}\kappa_{23}}{\mu^6}\right)^{\omega(t_1)} d_2 + \left(\frac{-s_2}{\mu^2}\right)^{\omega(t_2)-\omega(t_1)} \left(\frac{-s_{012}\kappa_{12}}{\mu^4}\right)^{\omega(t_1)-\omega(t_3)} \left(\frac{-s\kappa_{12}\kappa_{23}}{\mu^6}\right)^{\omega(t_3)} d_3 + \left(\frac{-s_2}{\mu^2}\right)^{\omega(t_2)-\omega(t_3)} \\ &\times \left(\frac{-s_{123}\kappa_{23}}{\mu^4}\right)^{\omega(t_3)-\omega(t_1)} \left(\frac{-s\kappa_{12}\kappa_{23}}{\mu^6}\right)^{\omega(t_1)} d_4 + \left(\frac{-s_3}{\mu^2}\right)^{\omega(t_3)-\omega(t_2)} \left(\frac{-s_1}{\mu^2}\right)^{\omega(t_1)-\omega(t_2)} \left(\frac{-s\kappa_{12}\kappa_{23}}{\mu^6}\right)^{\omega(t_2)} d_5 \end{aligned} \quad (66)$$

with the real coefficients $d_{i=1,2,3,4,5}$. Here

$$\kappa_{12} = (\vec{q}_1 - \vec{q}_2)^2, \quad \kappa_{23} = (\vec{q}_2 - \vec{q}_3)^2. \quad (67)$$

By comparing the above ‘‘dispersive’’ representation with the previous expressions for the BDS amplitude in the three physical regions Figs. 7(a)–7(c) it is possible to extract the coefficients. They read

$$\begin{aligned} d_1 &= c_1(\kappa_{12})c_1(\kappa_{23}), & d_2 &= c_2(\kappa_{12})c_2(\kappa_{23}), \\ d_3 + d_4 &= c_2(\kappa_{12})c_1(\kappa_{23}), & d_5 &= c_1(\kappa_{12})c_2(\kappa_{23}), \end{aligned} \quad (68)$$

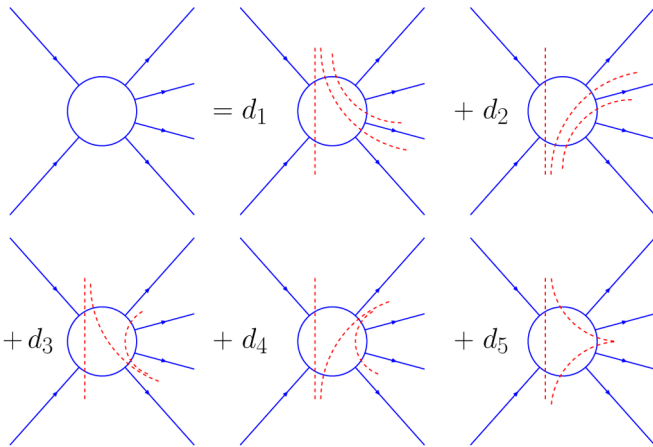


FIG. 8 (color online). Analytic representation of the amplitude $M_{2 \rightarrow 4}$.

$$s, s_{123}, s_1 > 0, \quad s_3, s_2, s_{012} < 0 \quad (64)$$

we have

$$\begin{aligned} \frac{M_{2 \rightarrow 4}}{\Gamma(t_1)\Gamma(t_3)} &= \left(\frac{-s_1}{\mu^2}\right)^{\omega(t_1)} \Gamma(t_2, t_1, \ln \kappa_{12} - i\pi) \\ &\times \left(\frac{-s_2}{\mu^2}\right)^{\omega(t_2)} \Gamma(t_3, t_2, \ln \kappa_{23} + i\pi) \\ &\times \left(\frac{-s_3}{\mu^2}\right)^{\omega(t_3)}. \end{aligned} \quad (65)$$

We can now attempt to write $M_{2 \rightarrow 4}$ in all physical regions in terms of the following dispersion ansatz (represented in Fig. 8)

where, in fact, $c_1(\kappa)$ and $c_2(\kappa)$ were defined in Eqs. (53) and (54):

$$c_1(\kappa_{12}) = |\Gamma_{12}| \frac{\sin \pi(\omega(t_1) - \phi_{\Gamma_{12}})}{\sin \pi(\omega(t_1) - \omega(t_2))}, \quad (69)$$

$$c_2(\kappa_{12}) = |\Gamma_{12}| \frac{\sin \pi(\omega(t_2) - \phi_{\Gamma_{12}})}{\sin \pi(\omega(t_2) - \omega(t_1))}, \quad (70)$$

$$c_1(\kappa_{23}) = |\Gamma_{23}| \frac{\sin \pi(\omega(t_2) - \phi_{\Gamma_{23}})}{\sin \pi(\omega(t_2) - \omega(t_3))}, \quad (71)$$

$$c_2(\kappa_{23}) = |\Gamma_{23}| \frac{\sin \pi(\omega(t_3) - \phi_{\Gamma_{23}})}{\sin \pi(\omega(t_3) - \omega(t_2))}, \quad (72)$$

with (cf. (49))

$$\Gamma_{12} = \Gamma(t_2, t_1, \ln -\kappa_{12}), \quad \Gamma_{23} = \Gamma(t_3, t_2, \ln -\kappa_{23}). \quad (73)$$

We note that for the coefficients d_3 and d_4 only their sum can be determined from the three physical regions previously discussed. However, an attempt to fix separately these two coefficients from the multi-Regge asymptotics in the physical region (see Fig. 7(d))

$$s, s_2 > 0, \quad s_1, s_3, s_{012}, s_{123} < 0$$

leads to a disaster: the corresponding equations do not have any solution. The reason for this is that the BDS amplitude in this region does not have the correct Regge factorization

(see the discussion in Sec. IV). According to Appendix C its asymptotics here is

$$\begin{aligned} \frac{M_{2 \rightarrow 4}}{\Gamma(t_1)\Gamma(t_3)} &= C \left(\frac{-s_1}{\mu^2}\right)^{\omega(t_1)} \Gamma(t_2, t_1, \ln \kappa_{12} - i\pi) \\ &\times \left(\frac{-s_2}{\mu^2}\right)^{\omega(t_2)} \Gamma(t_3, t_2, \ln \kappa_{23} - i\pi) \\ &\times \left(\frac{-s_3}{\mu^2}\right)^{\omega(t_3)}, \end{aligned} \quad (74)$$

where the coefficient C is given by

$$C = \exp\left[\frac{\gamma_K(a)}{4} i\pi \left(\ln \frac{\vec{q}_1^2 \vec{q}_3^2}{(\vec{k}_1 + \vec{k}_2)^2 \mu^2} - \frac{1}{\epsilon}\right)\right]. \quad (75)$$

The fact that, for this region, we find no solution for the coefficients d_i indicates that, in this region, the BDS amplitude does not have the correct analytic structure. In Sec. IV we will show, by comparing with explicit calculations of the high-energy limit of scattering amplitudes, that in the BDS formula a piece is missing. This piece belongs to a Regge-cut singularity, which—apart from the one-loop approximation—does not fit into the simple exponentiation of the BDS ansatz. In Appendix C we write down the amplitude $M_{2 \rightarrow 4}$ also in the quasi-multi-Regge kinematics, where the variable s_2 is fixed.

To continue our analysis of the BDS 6-point amplitude we now discuss the asymptotics of $M_{3 \rightarrow 3}$ (see Fig. 9). According to Appendix D in the multi-Regge region where all invariants $s, s_1, s_3, s_{13}, s_{02}, s_2 \equiv t_2'$ are large and negative, its asymptotics is similar to the corresponding asymptotics of the $M_{2 \rightarrow 4}$ amplitude, i.e.

$$\begin{aligned} \frac{M_{3 \rightarrow 3}}{\Gamma(t_1)\Gamma(t_3)} &= \left(\frac{-s_1}{\mu^2}\right)^{\omega(t_1)} \Gamma(t_2, t_1, \ln -\kappa_{12}) \\ &\times \left(\frac{-s_2}{\mu^2}\right)^{\omega(t_2)} \Gamma(t_3, t_2, \ln -\kappa_{23}) \left(\frac{-s_3}{\mu^2}\right)^{\omega(t_3)}. \end{aligned} \quad (76)$$

This BDS amplitude can be now analytically continued to the physical region where the invariants $s, s_1, s_3, s_{12}, s_{02}, t_2'$ are positive (see Fig. 10(a)). The resulting amplitude can be written as

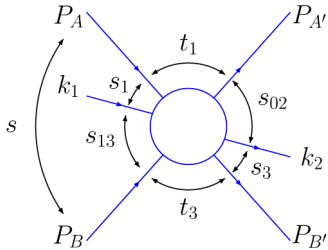


FIG. 9 (color online). Three particle transition.

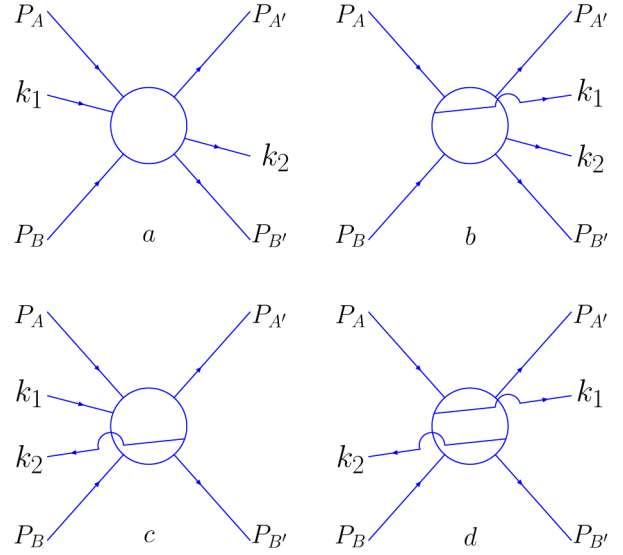


FIG. 10 (color online). Physical regions for the amplitude $M_{3 \rightarrow 3}$.

$$\begin{aligned} \frac{M_{3 \rightarrow 3}}{\Gamma(t_1)\Gamma(t_3)} &= \left(\frac{-s_1}{\mu^2}\right)^{\omega(t_1)} \Gamma(t_2, t_1, \ln \kappa_{12} - i\pi) \\ &\times \left(\frac{-s_2}{\mu^2}\right)^{\omega(t_2)} \Gamma(t_3, t_2, \ln \kappa_{23} - i\pi) \\ &\times \left(\frac{-s_3}{\mu^2}\right)^{\omega(t_3)}. \end{aligned} \quad (77)$$

Similarly, the analytic continuation to the region where $s_1, s_{12}, t_2' < 0$ and $s, s_3, s_{02} > 0$ (see Fig. 10(b)) is of the form

$$\begin{aligned} \frac{M_{3 \rightarrow 3}}{\Gamma(t_1)\Gamma(t_3)} &= \left(\frac{-s_1}{\mu^2}\right)^{\omega(t_1)} \Gamma(t_2, t_1, \ln \kappa_{12} + i\pi) \\ &\times \left(\frac{-s_2}{\mu^2}\right)^{\omega(t_2)} \Gamma(t_3, t_2, \ln \kappa_{23} - i\pi) \\ &\times \left(\frac{-s_3}{\mu^2}\right)^{\omega(t_3)}. \end{aligned} \quad (78)$$

Finally, the continuation to the region where $s_3, s_{02}, t_2' < 0$ and $s, s_1, s_{12} > 0$ (see Fig. 10(c)) reads

$$\begin{aligned} \frac{M_{3 \rightarrow 3}}{\Gamma(t_1)\Gamma(t_3)} &= \left(\frac{-s_1}{\mu^2}\right)^{\omega(t_1)} \Gamma(t_2, t_1, \ln \kappa_{12} - i\pi) \\ &\times \left(\frac{-s_2}{\mu^2}\right)^{\omega(t_2)} \Gamma(t_3, t_2, \ln \kappa_{23} + i\pi) \\ &\times \left(\frac{-s_3}{\mu^2}\right)^{\omega(t_3)}. \end{aligned} \quad (79)$$

As it was done in the $M_{2 \rightarrow 4}$ case one can write the dispersion relation for $M_{3 \rightarrow 3}$ valid in these physical regions, which includes five contributions, shown in Fig. 11, and calculate the real coefficients $e_1, e_2, e_3 + e_4, e_5$. But once again, we find that it is impossible to fix separately the coefficients e_3 and e_4 from the BDS amplitude, calculated

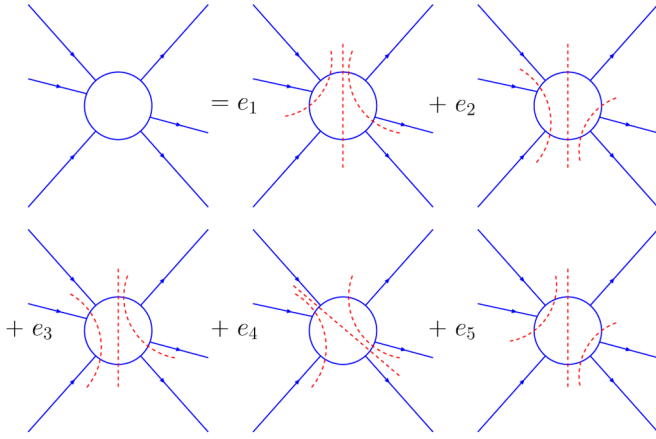


FIG. 11 (color online). Analytic representation of the amplitude $M_{3 \to 3}$.

in the physical region where $s_1, s_3, s_{13}, s_{02} < 0$ and $s, t'_2 > 0$ (see Fig. 10(d))

$$\begin{aligned} \frac{M_{3 \to 3}}{\Gamma(t_1)\Gamma(t_3)} &= C' \left(\frac{-s_1}{\mu^2}\right)^{\omega(t_1)} \Gamma(t_2, t_1, \ln \kappa_{12} + i\pi) \\ &\times \left(\frac{-s_2}{\mu^2}\right)^{\omega(t_2)} \Gamma(t_2, t_1, \ln \kappa_{23} + i\pi) \\ &\times \left(\frac{-s_3}{\mu^2}\right)^{\omega(t_3)}, \end{aligned} \quad (80)$$

where the phase factor C' is

$$C' = \exp\left[\frac{\gamma_K(a)}{4} (-i\pi) \ln \frac{(\vec{q}_1 - \vec{q}_2)^2 (\vec{q}_2 - \vec{q}_3)^2}{(\vec{q}_1 + \vec{q}_3 - \vec{q}_2)^2 \vec{q}_2^2}\right]. \quad (81)$$

The reason for this drawback is the same as before: the absence of a correct Regge factorization for the BDS amplitude. In the next section, using the BFKL approach,

we shall discuss the reason for this problem. Namely, the BDS amplitude does not contain the Mandelstam cut contributions plotted in Fig. 12.

IV. REGGE CUTS AND BREAKDOWN OF FACTORIZATION

A. Regge pole models

The results of the previous section can best be understood if we confront them with the known high-energy behavior of QCD scattering amplitudes in the Regge limit. In the LLA, the high-energy behavior of the QCD scattering amplitudes is the same as in the supersymmetric case. We proceed in three steps: we first review the findings for models containing only Regge poles. We then summarize the results obtained in gauge theories, and finally compare with the scattering amplitude derived from the BDS formula.

A key element in analyzing the high-energy limit are the Steinmann relations [39] which forbid the existence of simultaneous energy discontinuities in overlapping channels. As an illustrative example of the Steinmann relations, consider the $2 \rightarrow 3$ amplitude shown in Fig. 5: obviously, the produced particle in the central region can form resonance states with particle A' or with particle B' , but not simultaneously with both of them. As a result, in the physical region the scattering amplitude cannot have simultaneous discontinuities in the energy variables s_1 and s_2 . The way in which this restriction is implemented into scattering amplitudes is that, in the double Regge limit, the signated amplitude can be written as a sum of two pieces, one of them with cuts in the s_1 and in the s channels, the other one in the s_2 and in the s channels. In general, there are cut singularities both in the right and left half energy planes, and one has to form signated combinations.

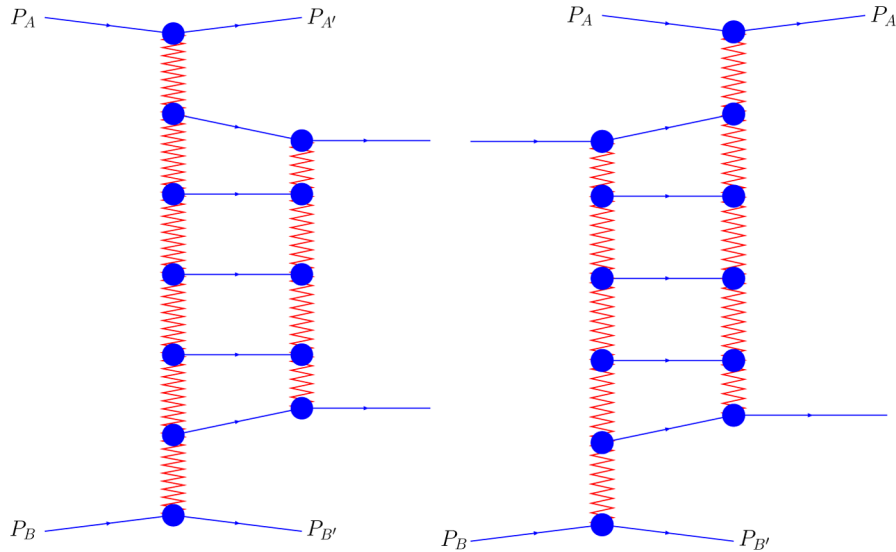


FIG. 12 (color online). BFKL contributions to the amplitudes $M_{2 \to 4}$ and $M_{3 \to 3}$.

Decompositions of this kind have first been derived from simple models which contain only Regge poles (massive scalar φ^3 theory [40] or the dual Veneziano 6 point amplitude, B_6 [41]), and from studies of dispersion relations and generalized Froissart-Gribov partial wave representations

$$\begin{aligned} \frac{A_{2 \rightarrow 3}}{\beta_A(t_1)\beta_B(t_2)} = & \left[\left(\frac{-s_1}{\mu^2} \right)^{\alpha(t_1) - \alpha(t_2)} + \tau_1 \tau_2 \left(\frac{s_1}{\mu^2} \right)^{\alpha(t_1) - \alpha(t_2)} \right] \left[\left(\frac{-s}{\mu^2} \right)^{\alpha(t_2)} + \tau_2 \left(\frac{s}{\mu^2} \right)^{\alpha(t_2)} \right] \tilde{V}_1(t_1, t_2, \kappa) \\ & + \left[\left(\frac{-s_2}{\mu^2} \right)^{\alpha(t_2) - \alpha(t_1)} + \tau_1 \tau_2 \left(\frac{s_2}{\mu^2} \right)^{\alpha(t_2) - \alpha(t_1)} \right] \left[\left(\frac{-s}{\mu^2} \right)^{\alpha(t_1)} + \tau_1 \left(\frac{s}{\mu^2} \right)^{\alpha(t_1)} \right] \tilde{V}_2(t_1, t_2, \kappa). \end{aligned} \quad (82)$$

Here $\alpha(t_i)$ denotes the trajectory function of the Regge pole in the t_i exchange channel, τ_1 (τ_2) are the signatures of the t_1 (t_2) channels, and as usual, $(-s)^\alpha = (|s|)^\alpha e^{-i\pi\alpha}$. In this representation, the energy singularities are explicit, i.e. all phase factors are contained in the energy factors, and the functions $\beta(t)$, V_i are real valued functions. With the abbreviations

$$\alpha_i = \alpha(t_i), \quad \alpha_{ij} = \alpha(t_i) - \alpha(t_j) \quad (83)$$

and with the signature factors

$$\xi_i = e^{-i\pi\alpha_i} + \tau_i, \quad \xi_{ij} = e^{-i\pi\alpha_{ij}} + \tau_i \tau_j \quad (84)$$

we can rewrite the expression for $A_{2 \rightarrow 3}$:

$$\begin{aligned} \frac{A_{2 \rightarrow 4}}{\beta_A(t_1)\beta_B(t_3)} = & \left(\frac{|s_1|}{\mu^2} \right)^{\alpha_{12}} \left(\frac{|s_{012}|}{\mu^2} \right)^{\alpha_{23}} \left(\frac{|s|}{\mu^2} \right)^{\alpha_3} \xi_{12} \xi_{23} \xi_3 \frac{V_1(t_1, t_2, \kappa_{12}) V_1(t_2, t_3, \kappa_{23})}{\sin \pi \alpha_{12} \sin \pi \alpha_{23}} \\ & + \left(\frac{|s_3|}{\mu^2} \right)^{\alpha_{32}} \left(\frac{|s_{123}|}{\mu^2} \right)^{\alpha_{21}} \left(\frac{|s|}{\mu^2} \right)^{\alpha_1} \xi_{32} \xi_{21} \xi_1 \frac{V_2(t_1, t_2, \kappa_{12}) V_2(t_2, t_3, \kappa_{23})}{\sin \pi \alpha_{32} \sin \pi \alpha_{21}} \\ & + \left(\frac{|s_2|}{\mu^2} \right)^{\alpha_{21}} \left(\frac{|s_{012}|}{\mu^2} \right)^{\alpha_{13}} \left(\frac{|s|}{\mu^2} \right)^{\alpha_3} \xi_{21} \xi_{13} \xi_3 \frac{\sin \pi \alpha_1}{\sin \pi \alpha_2} \frac{V_2(t_1, t_2, \kappa_{12}) V_1(t_2, t_3, \kappa_{23})}{\sin \pi \alpha_{21} \sin \pi \alpha_{13}} \\ & + \left(\frac{|s_2|}{\mu^2} \right)^{\alpha_{23}} \left(\frac{|s_{123}|}{\mu^2} \right)^{\alpha_{31}} \left(\frac{|s|}{\mu^2} \right)^{\alpha_1} \xi_{23} \xi_{31} \xi_1 \frac{\sin \pi \alpha_3}{\sin \pi \alpha_2} \frac{V_2(t_1, t_2, \kappa_{12}) V_1(t_2, t_3, \kappa_{23})}{\sin \pi \alpha_{23} \sin \pi \alpha_{31}} \\ & + \left(\frac{|s_3|}{\mu^2} \right)^{\alpha_{32}} \left(\frac{|s_1|}{\mu^2} \right)^{\alpha_{12}} \left(\frac{|s|}{\mu^2} \right)^{\alpha_2} \xi_{32} \xi_{12} \xi_2 \frac{V_1(t_1, t_2, \kappa_{12}) V_2(t_2, t_3, \kappa_{23})}{\sin \pi \alpha_{32} \sin \pi \alpha_{12}}. \end{aligned} \quad (86)$$

The analogue for the $3 \rightarrow 3$ process again consists of five pieces which are shown in Fig. 11.

From the discussions of these Regge pole models it has also been recognized that the analytic decomposition into a sum of terms in (85) and (86) is consistent with a factorizing form. For the $2 \rightarrow 3$ case we can write:

$$\frac{A_{2 \rightarrow 3}}{\beta_A(t_1)\beta_B(t_2)} = \left(\frac{|s_1|}{\mu^2} \right)^{\alpha_1} \xi_1 V_{\tau_1 \tau_2}(t_1, t_2, \kappa) \left(\frac{|s_2|}{\mu^2} \right)^{\alpha_2} \xi_2. \quad (87)$$

Here the important point to be stressed is that the new production vertex function $V_{\tau_1 \tau_2}$ contains phases (in contrast to the real-valued functions V_i in (85)), and it has cut singularities in the κ -plane. Similarly for the $2 \rightarrow 4$ case

[42]. For $2 \rightarrow 4$ or $3 \rightarrow 3$ amplitudes, we have five independent terms, and for scattering processes with a higher number of legs the number of terms grows rapidly.

For models which contain only Regge poles the general structure of the signed $2 \rightarrow 3$ amplitude is

$$\begin{aligned} \frac{A_{2 \rightarrow 3}}{\beta_A(t_1)\beta_B(t_2)} = & \left(\frac{|s_1|}{\mu^2} \right)^{\alpha_{12}} \left(\frac{|s|}{\mu^2} \right)^{\alpha_2} \xi_{12} \xi_2 \frac{V_1(t_1, t_2, \kappa)}{\sin \pi \alpha_{12}} \\ & + \left(\frac{|s_2|}{\mu^2} \right)^{\alpha_{21}} \left(\frac{|s|}{\mu^2} \right)^{\alpha_1} \xi_{21} \xi_1 \frac{V_2(t_1, t_2, \kappa)}{\sin \pi \alpha_{21}}, \end{aligned} \quad (85)$$

where the vertex function V_i is proportional to \tilde{V}_i . The generalization to the signed $2 \rightarrow 4$ amplitude (consisting of five different pieces) is illustrated in Fig. 8, and from Eq. (66) one easily obtains the analogue of (85) [41]:

we have

$$\begin{aligned} \frac{A_{2 \rightarrow 4}}{\beta_A(t_1)\beta_B(t_3)} = & \xi_1 \left(\frac{|s_1|}{\mu^2} \right)^{\alpha_1} V_{\tau_1 \tau_2}(t_1, t_2, \kappa_{12}) \\ & \times \xi_2 \left(\frac{|s_2|}{\mu^2} \right)^{\alpha_2} V_{\tau_2 \tau_3}(t_2, t_3, \kappa_{23}) \xi_3 \left(\frac{|s_3|}{\mu^2} \right)^{\alpha_3} \end{aligned} \quad (88)$$

with the production vertex function from (87). As a result, for this class of Regge pole models the production amplitudes, in the multi-Regge limit, can be written either in the ‘‘analytic’’ form (sum of terms with simple analytic properties and real-valued vertex functions V_i) or in the ‘‘fac-

torized” form (with the production vertices V containing phases and singularities in κ).

Let us comment on the planar approximation. Planar amplitudes have right-hand cut singularities only, and in the physical region where all energies are positive, their phases follow from the signatured amplitudes in (85) or (86) by simply dropping all “twisted” terms containing factors τ_i . One can easily verify that, in the physical region where all energies are positive, these planar amplitudes can also be written in the factorized form (87) and (88) (with vertex functions $V(t_1, t_2, \kappa_{12})$ being slightly different from the signatured ones, $V_{\tau_1\tau_2}(t_1, t_2, \kappa_{12})$). When analytically continuing into the unphysical region, where all energy variables are negative and well separated from their threshold singularities, all phases inside the production vertex $V(t_1, t_2, \kappa_{12})$ disappear, the vertex function turns into a real-valued function, and the factorized form remains valid. However, in the physical region where $s, s_2 > 0$ and $s_1, s_3, s_{012}, s_{123} < 0$ the factorized form is not valid, and the structure of the amplitude is more complicated.

B. High-energy behavior in Yang-Mills theories

Let us now turn to QCD. Throughout this section we will restrict ourselves to scattering amplitudes with odd signature in all t -channels. Compared to the Regge pole models discussed in the previous subsection, the situation is slightly more complicated since also Regge cut pieces appear in some of the t -channels. In the LLA the real part of the $2 \rightarrow n$ scattering amplitude is well known to have the factorized form of Eq. (4), and it is in agreement with our previous result in (87) and (88). However, when turning to the imaginary parts (i.e. to the energy discontinuities) of the production amplitudes, a new piece appears which destroys the simple factorization property. The best way of understanding the appearance of this new piece is the use of s -channel unitarity in the physical region where all energies are positive.

Starting from the analytic representation of the scattering amplitude $A_{2 \rightarrow n}$, it is possible to determine, in QCD, the partial waves from energy discontinuities and unitarity equations [43,44]. As the simplest example, let us consider, in the LLA, the $2 \rightarrow 3$ amplitude, consisting of the two terms illustrated in Fig. 5. Anticipating that, in the $2 \rightarrow 3$ process, there are only Regge pole contributions, we start from the ansatz

$$\begin{aligned} \frac{A_{2 \rightarrow 3}}{\Gamma(t_1)\Gamma(t_2)} &= \frac{2s}{t_1 t_2} \left[\left(\frac{|s_1|}{\mu^2} \right)^{\omega_{12}} \left(\frac{|s|}{\mu^2} \right)^{\omega_2} \xi_{12} \xi_2 \frac{V_1(t_1, t_2, \kappa)}{\sin \pi \omega_{12}} \right. \\ &\quad \left. + \left(\frac{|s_2|}{\mu^2} \right)^{\omega_{21}} \left(\frac{|s|}{\mu^2} \right)^{\omega_1} \xi_{21} \xi_1 \frac{V_2(t_1, t_2, \kappa)}{\sin \pi \omega_{21}} \right] \end{aligned} \quad (89)$$

with (cf. (56))

$$\kappa = (\vec{q}_1 - \vec{q}_2)^2 \quad (90)$$

and

$$\Gamma(t_1) = g \delta_{\lambda_A \lambda_{A'}}, \quad \Gamma(t_2) = g \delta_{\lambda_B \lambda_{B'}}. \quad (91)$$

Here we used $\alpha_i(t_i) = 1 + \omega(t_i)$ and

$$\omega_i = \omega(t_i), \quad \omega_{ij} = \omega(t_i) - \omega(t_j), \quad (92)$$

and the signature factors can be written in following form:

$$\xi_i = e^{-i\pi\omega_i} + 1, \quad \xi_{ij} = e^{-i\pi\omega_{ij}} + 1. \quad (93)$$

Taking the discontinuity in s_1 , only the first term in (89) contributes. Making use of the unitarity equation and invoking, for the ladder diagrams in the t_1 channel, the BFKL bootstrap condition we find the partial wave V_1 in the LLA. For a definite helicity V_1 has the form

$$V_1 = g\pi C(q_2, q_1) \left(\frac{1}{2}(\omega_1 - \omega_2) - \frac{a}{2} \left(\ln \frac{\kappa}{\mu^2} - \frac{1}{\epsilon} \right) \right) \quad (94)$$

with $C(q_2, q_1)$ being the production vertex from (6). Similarly, the discontinuity in s_2 leads to

$$V_2 = g\pi C(q_2, q_1) \left(\frac{1}{2}(\omega_2 - \omega_1) - \frac{a}{2} \left(\ln \frac{\kappa}{\mu^2} - \frac{1}{\epsilon} \right) \right). \quad (95)$$

A comment may be in place on the term $\ln \kappa$ in V_1 and V_2 : it indicates that, in contrast to massive field theories where the V_i 's are analytic functions near $\kappa = 0$, in massless theories this is no longer the case. Therefore, when computing the discontinuity in s_1 or s_2 of $A_{2 \rightarrow 3}$, there is, at first sight, an uncertainty in handling the cut in κ . It turns out that the correct prescription for computing the discontinuity in s_1 or s_2 in the physical region, is keeping $\kappa = (\vec{q}_1 - \vec{q}_2)^2$ fixed. This can be derived either from a direct analysis of Feynman diagrams where the Steinmann relations $\text{disc}_{s_1} \text{disc}_{s_2} A_{2 \rightarrow 3} = 0$ are fulfilled explicitly. Alternatively, one can consider the massless Yang-Mills theory as the zero mass limit of anon-Abelian Higgs model where the gauge bosons are massive: before the zero mass limit is taken, the vertex functions are analytic near $\kappa = 0$ and there is no ambiguity in computing the energy discontinuities. As a result, in the physical region the singularities in κ of V_1 and V_2 are not related to singularities in s_1 or s_2 . We also mention that, in the next-to-leading approximation, the functions V_1 and V_2 contain an additional dependence on $\ln \kappa$, which, again, does not contradict the Steinmann relations [33].

Inserting these expressions into Eq. (89), using (93), and restricting ourselves to the planar approximation, we find for the real part (apart from the color factor):

$$\frac{A_{2 \rightarrow 3}}{\Gamma(t_1)\Gamma(t_2)} = \frac{2s}{t_1 t_2} (|s_1|)^{\omega_1} g C(q_2, q_1) (|s_2|)^{\omega_2} \quad (96)$$

in agreement with (4). In particular, the infrared singular pieces in V_1 and V_2 cancel. As a further test, one could also compute, from the corresponding unitarity equation, the single discontinuity in s : here both partial waves V_1 and

V_2 contribute, and the result is in agreement with (94) and (95).³

For the $2 \rightarrow 4$ amplitude we start from an ansatz which is slightly more general than (86). In order to account for

the Regge cut in the t_2 channel, we introduce, in the t_2 -channel, the Sommerfeld-Watson integral $\int d\omega'_2/2\pi i$:

$$\begin{aligned} \frac{A_{2 \rightarrow 4}}{\Gamma(t_1)\Gamma(t_3)} = & \frac{2s}{t_1 t_2 t_3} \int \frac{d\omega'_2}{2\pi i} \left[\left(\frac{|s_1|}{\mu^2} \right)^{\omega_1 - \omega'_2} \left(\frac{|s_{012}|}{\mu^2} \right)^{\omega'_2 - \omega_3} \left(\frac{|s|}{\mu^2} \right)^{\omega_3} \xi_{12'} \xi_{2'3} \xi_3 \frac{W_1(t_1, t_2, t_3, \kappa_{12}, \kappa_{23}; \omega'_2)}{\sin \pi \omega_{12'} \sin \pi \omega_{2'3}} \right. \\ & + \left(\frac{|s_3|}{\mu^2} \right)^{\omega_3 - \omega'_2} \left(\frac{|s_{123}|}{\mu^2} \right)^{\omega'_2 - \omega_1} \left(\frac{|s|}{\mu^2} \right)^{\omega_1} \xi_{32'} \xi_{2'1} \xi_1 \frac{W_2(t_1, t_2, t_3, \kappa_{12}, \kappa_{23}; \omega'_2)}{\sin \pi \omega_{32'} \sin \pi \omega_{2'1}} \\ & + \left(\frac{|s_2|}{\mu^2} \right)^{\omega'_2 - \omega_1} \left(\frac{|s_{012}|}{\mu^2} \right)^{\omega_1 - \omega_3} \left(\frac{|s|}{\mu^2} \right)^{\omega_3} \xi_{2'1} \xi_{13} \xi_3 \frac{W_3(t_1, t_2, t_3, \kappa_{12}, \kappa_{23}, \kappa_{123}; \omega'_2)}{\sin \pi \omega_{2'1} \sin \pi \omega_{13}} \\ & + \left(\frac{|s_2|}{\mu^2} \right)^{\omega'_2 - \omega_3} \left(\frac{|s_{123}|}{\mu^2} \right)^{\omega_3 - \omega_1} \left(\frac{|s|}{\mu^2} \right)^{\omega_1} \xi_{2'3} \xi_{31} \xi_1 \frac{W_4(t_1, t_2, t_3, \kappa_{12}, \kappa_{23}, \kappa_{123}; \omega'_2)}{\sin \pi \omega_{2'3} \sin \pi \omega_{31}} \\ & \left. + \left(\frac{|s_3|}{\mu^2} \right)^{\omega_3 - \omega'_2} \left(\frac{|s_1|}{\mu^2} \right)^{\omega_1 - \omega'_2} \left(\frac{|s|}{\mu^2} \right)^{\omega_2} \xi_{32'} \xi_{12'} \xi_{2'} \frac{W_5(t_1, t_2, t_3, \kappa_{12}, \kappa_{23}; \omega'_2)}{\sin \pi \omega_{32'} \sin \pi \omega_{12'}} \right]. \end{aligned} \quad (97)$$

with the partial wave functions, denoted by $W_{i=1,2,3,4,5}$ and to be determined from single energy discontinuity equations. The partial wave functions W_3 and W_4 also depend upon the additional variable $\kappa_{123} = (\vec{k}_1 + \vec{k}_2)^2$. We have the five single discontinuities in s_1 , s_2 , s_3 , s_{012} , and s_{123} which allow to find the partial waves $W_{i=1,2,3,4,5}$. In leading log accuracy the results are the following:

$$W_1 = V_1(t_1, t_2, \kappa_{12}) \frac{1}{\omega'_2 - \omega_2} V_1(t_2, t_3, \kappa_{23}), \quad (98)$$

$$W_2 = V_2(t_1, t_2, \kappa_{12}) \frac{1}{\omega'_2 - \omega_2} V_2(t_2, t_3, \kappa_{23}), \quad (99)$$

$$\begin{aligned} W_3 = & \frac{\sin \pi \omega_1}{\sin \pi \omega_2} V_2(t_1, t_2, \kappa_{12}) \frac{1}{\omega'_2 - \omega_2} V_1(t_2, t_3, \kappa_{23}) \\ & - \sin \pi (\omega'_2 - \omega_1) (V_{\text{cut}} - V_p), \end{aligned} \quad (100)$$

$$\begin{aligned} W_4 = & \frac{\sin \pi \omega_3}{\sin \pi \omega_2} V_2(t_1, t_2, \kappa_{12}) \frac{1}{\omega'_2 - \omega_2} V_1(t_2, t_3, \kappa_{23}) \\ & - \sin \pi (\omega'_2 - \omega_3) (V_{\text{cut}} - V_p), \end{aligned} \quad (101)$$

$$W_5 = V_1(t_1, t_2, \kappa_{12}) \frac{1}{\omega'_2 - \omega_2} V_2(t_2, t_3, \kappa_{23}). \quad (102)$$

The three amplitudes W_1 , W_2 and W_5 are products of the production vertices V_i in (94) and (95), found in the $2 \rightarrow 3$ case, whereas the amplitudes W_3 and W_4 contain, in addition to the products of production vertices V_i , the extra pieces, $V_{\text{cut}} - V_p$ which will be defined in the following.

³We emphasize that the same results are obtained if one starts from the double discontinuities in s and s_1 : using unitarity conditions and making use of generalized bootstrap conditions, one again arrives at (94). This is a crucial test of the self-consistency of this ‘‘unitarity-based approach.’’

The term V_{cut} contains Regge cuts and cannot be written as a simple product of vertices for the two produced gluons. It takes the form of BFKL-like ladder diagrams in the color octet channel, and it is illustrated in Fig. 12 (left figure):

$$\begin{aligned} V_{\text{cut}} = & \frac{t_2 N_c}{2} g^4 \int \frac{d^2 k d^2 k'}{(2\pi)^6} \frac{q_1^2}{(k + k_1)^2} C(k, k + k_1) \\ & \times G^{(8_A)}(k, q_2 - k; k', q_2 - k'; \omega'_2) C(k' - k_2, k') \\ & \times \frac{q_3^2}{(k' - k_2)^2}. \end{aligned} \quad (103)$$

Here C denotes the effective Reggeon-Reggeon-gluon vertex given in (6), and $G^{(8_A)}$ is the BFKL Green's function in the color octet channel, satisfying the integral equation

$$\begin{aligned} & \omega'_2 G^{(8_A)}(k, q - k; k', q - k'; \omega'_2) \\ & = \frac{(2\pi)^3 \delta^{(2)}(k - k')}{k^2 (q - k)^2} + \frac{1}{k^2 (q - k)^2} \\ & \times (K \otimes G^{(8_A)})(k, q - k; k', q - k'), \end{aligned} \quad (104)$$

where K denotes the BFKL kernel in the color octet channel, containing both real emission and the gluon trajectory. In lowest order in the coupling, and for equal helicities of the two produced gluons, V_{cut} equals:

$$V_{\text{cut}}^{(0)} = g^2 \frac{C(q_2, q_1) C(q_3, q_2)}{2\omega'_2} \left[\omega_1 + \omega_3 + a \left(\ln \frac{\kappa_{123}}{\mu^2} - \frac{1}{\epsilon} \right) \right]. \quad (105)$$

The term V_{cut} not only violates the simple factorization of Regge pole models, but also, when computed beyond the one-loop approximation, will be shown to disagree with the BDS formula. Finally, the subtraction term V_p removes the Regge pole piece inside V_{cut} , and it is of the form:

$$V_p = g^2 \frac{C(q_2, q_1)C(q_3, q_2)}{4\omega_2} \left[\omega_1 + \omega_2 + a \left(\ln \frac{\kappa_{12}}{\mu^2} - \frac{1}{\epsilon} \right) \right] \times \frac{1}{\omega'_2 - \omega_2} \cdot \left[\omega_2 + \omega_3 + a \left(\ln \frac{\kappa_{23}}{\mu^2} - \frac{1}{\epsilon} \right) \right]. \quad (106)$$

Before we compare with the BDS formula, let us remark on a few features of these leading order QCD results (for details, see Appendix E). From now on, we specialize on the planar approximation, i.e. in the signature factors in Eq. (93) we only retain the phases. Inserting the results of (98)–(102) into the full amplitude (97) we can derive the results for different kinematic regions.

Beginning with the physical region where all energies are positive, one finds that the sum of the Regge pole terms can be written in the simple factorizing form (88). In particular, the Regge cut pieces contained in W_3 and W_4 cancel completely, and the real part of the scattering amplitude coincides with (4).

Next, in the unphysical region where all energies are negative and all phases disappear, again, the Regge pole contributions can be written in a simple factorizing form, and the cut pieces in W_3 and W_4 cancel.

Finally, we go into the physical region where $s, s_2 > 0$ and $s_1, s_3, s_{012}, s_{123} < 0$. Nonzero phases appear only in s and in s_2 . After some algebra we obtain:

$$\frac{A_{2 \rightarrow 4}}{\Gamma(t_1)\Gamma(t_3)} = \frac{2s}{t_1 t_2 t_3} g^2 C(q_2, q_1) C(q_3, q_2) (|s_1|)^{\omega_1} (|s_3|)^{\omega_3} \cdot e^{-i\pi\omega_2} (|s_2|)^{\omega_2} \left[1 + i \frac{\pi}{2} \left(\omega_1 + \omega_2 + a \left(\ln \frac{\kappa_{12}}{\mu^2} - \frac{1}{\epsilon} \right) + \omega_3 + \omega_2 + a \left(\ln \frac{\kappa_{23}}{\mu^2} - \frac{1}{\epsilon} \right) \right) \right] - 2i\pi \frac{2s}{t_1 t_2 t_3} \int \frac{d\omega'_2}{2\pi i} (e^{-i\pi|s_2|})^{\omega'_2} V_{\text{cut}}. \quad (107)$$

In the last term, V_{cut} , it is possible to factor out the gluon trajectory (details are presented in [45]):

$$\int \frac{d\omega'_2}{2\pi i} (e^{-i\pi|s_2|})^{\omega'_2} V_{\text{cut}} = g^2 C(q_2, q_1) C(q_3, q_2) (e^{-i\pi|s_2|})^{\omega_2} \times \int \frac{d\omega'_2}{2\pi i} (e^{-i\pi|s_2|})^{\omega'_2} V_{\text{cut, reduced}}, \quad (108)$$

where in the one-loop approximation (105)

$$g^2 C(q_2, q_1) C(q_3, q_2) \int \frac{d\omega'_2}{2\pi i} (e^{-i\pi|s_2|})^{\omega'_2} V_{\text{cut, reduced}} = g^2 \frac{C(q_2, q_1) C(q_3, q_2)}{2} \left[a \left(\ln \frac{\kappa_{123}\mu^2}{q_1^2 q_3^2} + \frac{1}{\epsilon} \right) + \mathcal{O}(a^2 \ln s_2) \right], \quad (109)$$

and the two-loop and higher order terms of $V_{\text{cut, reduced}}$ are infrared finite [45].

Inserting (108) into (107) we see that all terms on the right-hand side of (107) are proportional to the common phase factor $e^{-i\pi\omega_2}$:

$$\frac{A_{2 \rightarrow 4}}{\Gamma(t_1)\Gamma(t_3)} = \frac{2s}{t_1 t_2 t_3} (|s_1|)^{\omega_1} (|s_3|)^{\omega_3} (|s_2|)^{\omega_2} g^2 C(q_2, q_1) \times C(q_3, q_2) e^{-i\pi\omega_2} \cdot \left[1 + i \frac{\pi}{2} \left(\omega_1 + \omega_2 + a \left(\ln \frac{\kappa_{12}}{\mu^2} - \frac{1}{\epsilon} \right) + \omega_3 + \omega_2 + a \left(\ln \frac{\kappa_{23}}{\mu^2} - \frac{1}{\epsilon} \right) \right) - 2i\pi \int \frac{d\omega'_2}{2\pi i} (e^{-i\pi|s_2|})^{\omega'_2} V_{\text{cut, reduced}} \right], \quad (110)$$

and the coefficient in the square brackets is infrared finite. This shows that, in LLA, the imaginary part of $A_{2 \rightarrow 4}$ is infrared singular, but the singularities are assembled in the phase factor $e^{-i\pi\omega_2}$. This observation will be important when comparing with the BDS formula.

A completely analogous discussion applies to the case $3 \rightarrow 3$ (Figs. 9 and 11) in the multi-Regge region (a more detailed discussion is given in Appendix E). Again, the scattering amplitude consists of five terms, and two of them contain the Regge cut piece:

$$\int \frac{d\omega'_2}{2\pi i} (e^{-i\pi|s_2|})^{\omega'_2} U_{\text{cut}}$$

with

$$U_{\text{cut}} = \frac{t_2 N_c}{2} g^4 \int \frac{d^2 k d^2 k'}{(2\pi)^6} \frac{q_1^2}{(k - q_1)^2} C(q_2 - k, q_1 - k) \times G^{(8_A)}(k, q_2 - k; k', q_2 - k'; \omega'_2) C(k' - k_2, k') \times \frac{q_3^2}{(k' - k_2)^2}. \quad (111)$$

In lowest order (and for equal helicities of the produced gluons) this Regge cut piece equals:

$$U_{\text{cut}}^{(0)} = \frac{g^2 C(q_2, q_1) C(q_3, q_2)}{2\omega'_2} a \ln \frac{\kappa_{12}\kappa_{23}}{(\tilde{q}_1 + \tilde{q}_3 - \tilde{q}_2)^2 q_2^2}. \quad (112)$$

Proceeding in the same way as for the $2 \rightarrow 4$ amplitude, one derives results for the scattering amplitude in the different kinematic regions. In the region where all energies are positive, we find the same factorization as for simple Regge pole models, i.e. the Regge cut pieces cancel. In the region $s, s_2 > 0, s_1, s_3, s_{13}, s_{02} < 0$ the Regge cut piece

appears. First we rewrite it in the same form as in (108):

$$\begin{aligned} & \int \frac{d\omega'_2}{2\pi i} (e^{-i\pi|s_2|})^{\omega'_2} U_{\text{cut}} \\ &= g^2 C(q_2, q_1) C(q_3, q_2) (e^{-i\pi|s_2|})^{\omega_2} \\ & \quad \times \int \frac{d\omega'_2}{2\pi i} (e^{-i\pi|s_2|})^{\omega'_2} U_{\text{cut, reduced}} \end{aligned} \quad (113)$$

with the infrared finite one-loop approximation

$$\begin{aligned} & g^2 C(q_2, q_1) C(q_3, q_2) \int \frac{d\omega'_2}{2\pi i} (e^{-i\pi|s_2|})^{\omega'_2} U_{\text{cut, reduced}} \\ &= g^2 \frac{C(q_2, q_1) C(q_3, q_2)}{2} \left[a \left(\ln \frac{\kappa_{12} \kappa_{23}}{(\vec{q}_1 + \vec{q}_3 - \vec{q}_2)^2 q_2^2} \right) \right. \\ & \quad \left. + \mathcal{O}(a^2 \ln s_2) \right]. \end{aligned} \quad (114)$$

As in the case of the $2 \rightarrow 4$ amplitude, the higher order corrections (denoted by $\mathcal{O}(a^2)$) are infrared finite. With this result, the $3 \rightarrow 3$ amplitude can be written in the form (cf. (110)):

$$\begin{aligned} \frac{A_{3 \rightarrow 3}}{\Gamma(t_1) \Gamma(t_3)} &= \frac{2s}{t_1 t_2 t_3} (|s_1|)^{\omega_1} (|s_2|)^{\omega_2} \\ & \quad \times (|s_3|)^{\omega_3} g^2 C(q_2, q_1) C(q_3, q_2). \end{aligned}$$

$$\begin{aligned} & \left[1 + i \frac{\pi}{2} \left(\omega_1 + a \left(\ln \frac{\kappa_{12}}{\mu^2} - \frac{1}{\epsilon} \right) + \omega_3 + a \left(\ln \frac{\kappa_{23}}{\mu^2} - \frac{1}{\epsilon} \right) \right) \right. \\ & \quad \left. - 2i\pi \int \frac{d\omega'_2}{2\pi i} (e^{-i\pi|s_2|})^{\omega'_2} U_{\text{cut, reduced}} \right]. \end{aligned} \quad (115)$$

Note that, in contrast to the $2 \rightarrow 4$ case, there is no common infrared singular phase factor, $e^{-i\pi\omega_2}$, and the square bracket term on the right-hand side of (115) is infrared finite. This shows that the infrared structure of $A_{3 \rightarrow 3}$ is quite different from $A_{2 \rightarrow 4}$.

C. Comparison with the BDS formula

Let us now return to the BDS amplitude discussed in Sec. III, take the leading logarithmic approximation and compare with the results discussed in the previous subsection. In the leading logarithmic approximation we retain, in the exponent $\ln M_n$, only the lowest order (in powers of a) of the coefficients of the energy logarithms, and the lowest order of the real and imaginary parts of logarithms of the vertex functions, $\ln \Gamma$. In the case of the $2 \rightarrow 2$ scattering process the coefficient of $\ln s$ is given by the gluon trajectory function (Eq. (38)), and the leading order coefficient is the term proportional to a . The logarithm of the vertex function is given in (39); the lowest order term is of order a , and since t is negative, there is no imaginary part. Therefore, in the leading logarithmic approximation we

put $\ln \Gamma$ equal to zero (note that M_4 multiplies the Born approximation which contains a Reggeon-particle-particle vertex of the order g).

Turning to the case $2 \rightarrow 3$ in the physical region, we use (46) and (49) (see also Appendix B). The new element, the logarithm of the production vertex, starts with terms of the order a , and the real part can be neglected (i.e. the absolute value of $\Gamma(t_2, t_1, \kappa)$ can be put equal to unity). But, depending upon the kinematic region, terms with $\ln(-\kappa)$ may lead to imaginary parts of order a which have to be kept. In the region where all energies are positive the relevant terms of order a are (see (55)):

$$\Phi_\Gamma = \frac{1}{2} (\omega(t_1) + \omega(t_2)) + \frac{a}{2} \left(\ln \frac{\kappa}{\mu^2} - \frac{1}{\epsilon} \right). \quad (116)$$

In order to compare with the QCD results we use (52)–(54). In (52) we approximate the factors $\kappa^{\omega(t_i)} \rightarrow 1$ etc., and for the real coefficients c_1 and c_2 we obtain:

$$\begin{aligned} c_1 &= \frac{\frac{1}{2} (\omega(t_1) - \omega(t_2) - a (\ln \frac{\kappa}{\mu^2} - \frac{1}{\epsilon}))}{\omega(t_1) - \omega(t_2)}, \\ c_2 &= \frac{\frac{1}{2} (\omega(t_2) - \omega(t_1) - a (\ln \frac{\kappa}{\mu^2} - \frac{1}{\epsilon}))}{\omega(t_2) - \omega(t_1)} \end{aligned} \quad (117)$$

which agrees with the leading log result in (89), (94), and (95). In the unphysical region where all energies are negative we have no imaginary parts and again find complete agreement with the results of the previous subsection.

In the case of $2 \rightarrow 4$ we begin with the physical region where all energies are positive. Using Eqs. (66)–(68) and applying the same arguments as for the $2 \rightarrow 3$ case, we find

$$\begin{aligned} \frac{M_{2 \rightarrow 4}}{\Gamma(t_1) \Gamma(t_3)} &= \left(e^{-i\pi} \frac{|s_1|}{\mu^2} \right)^{\omega_1} (c_1(\kappa_{12}) + c_2(\kappa_{12})) \\ & \quad \times \left(e^{-i\pi} \frac{|s_2|}{\mu^2} \right)^{\omega_2} (c_1(\kappa_{23}) + c_2(\kappa_{23})) \\ & \quad \times \left(e^{-i\pi} \frac{|s_3|}{\mu^2} \right)^{\omega_3}, \end{aligned} \quad (118)$$

quite in agreement with the LLA of the Regge pole part in (E3). Since, in the QCD calculation for this kinematic region, the Regge cut pieces cancel, there is no conflict between the BDS formula and the leading logarithmic approximation obtained by direct calculations.

Let us now turn to the region $s, s_2 > 0, s_1, s_{012}, s_{123}, s_3 < 0$ where, in the QCD calculations, the imaginary part contains the factorization breaking term V_{cut} (corresponding to a BFKL ladder with the octet quantum numbers in the t -channel). In the BDS amplitude (74) we have, compared to the physical region with only positive energies, the additional phase factor C in (75). In the leading log approximation which we have described before we find (from (74) and (75), or from (C11)):

$$\frac{M_{2 \rightarrow 4}}{\Gamma(t_1)\Gamma(t_3)} = \left(\frac{|s_1|}{\mu^2}\right)^{\omega_1} \left(\frac{|s_3|}{\mu^2}\right)^{\omega_3} \left(e^{-i\pi} \frac{|s_2|}{\mu^2}\right)^{\omega_2} \cdot \left[1 + i\frac{\pi}{2} \left(\omega_1 + \omega_2 + a \left(\ln \frac{\kappa_{12}}{\mu^2} - \frac{1}{\epsilon} \right) + \omega_3 + \omega_2 + a \left(\ln \frac{\kappa_{23}}{\mu^2} - \frac{1}{\epsilon} \right) \right) + i\pi a \left(\ln \frac{q_1^2 q_3^2}{(k_1 + k_2)^2 \mu^2} - \frac{1}{\epsilon} \right) \right]. \quad (119)$$

In the imaginary part of the square brackets the ϵ poles cancel. Comparing this result with (110) and (105) we see that the BDS formula reproduces the lowest order term of the Regge cut contribution, $V_{\text{cut, reduced}}$, but not the higher order terms (which are still part of the leading logarithmic approximation). We therefore conclude that, beyond the one-loop approximation, the BDS formula does not agree with the leading log results listed in the previous subsection.

Let us remark on the order $\mathcal{O}(\epsilon)$ corrections in the BDS formula. As explained at the beginning of Sec. III, our analysis of the BDS formula (which applies to the logarithm of the scattering amplitude) does not include terms which vanish as $\epsilon \rightarrow 0$. Nevertheless, the comparison of (110) and (119) shows that such corrections cannot reproduce the finite (in ϵ) terms which are missing in the BDS formula. The key point is that, in the BDS formula, the leading log approximation for the imaginary part of $\ln M_{2 \rightarrow 4}$ contains terms of the order $1/\epsilon$ only inside ω_2 . Comparing (110) with (119) one sees that the infrared divergent phase factor for the cut contribution in (110) is the same as in the BDS formula. Therefore, when going from $\ln M_{2 \rightarrow 4}$ to $M_{2 \rightarrow 4}$ it is incorrect to expand this infrared singular piece $e^{-i\pi a/\epsilon}$, and it becomes clear that terms of order ϵ in the logarithm of the scattering amplitude cannot produce constant (in ϵ) terms in the scattering amplitude. As a result, our conclusion concerning the validity of the BDS formula is not affected by the order $\mathcal{O}(\epsilon)$ corrections in the BDS formula for the logarithm of the scattering amplitude.

For the $3 \rightarrow 3$ amplitude the comparison between the BDS amplitude and the high-energy behavior in Yang-Mills theories leads to the same conclusion, although some details are different. For the kinematic region where all energies are positive the BDS formula agrees with the leading log calculations, and we directly turn to the region $s, s_2 > 0, s_1, s_3, s_{13}, s_{02} < 0$. The crucial element is the phase C' in (81) which, in contrast to C in (75), is infrared finite. Collecting, in (80) and (81), or in (D8), within LLA, all imaginary parts in $\ln M_{3 \rightarrow 3}$ we note that all terms of the form a/ϵ cancel, and we arrive at:

$$\frac{M_{3 \rightarrow 3}}{\Gamma(t_1)\Gamma(t_3)} = \left(\frac{|s_1|}{\mu^2}\right)^{\omega_1} \left(\frac{|s_3|}{\mu^2}\right)^{\omega_3} \left(\frac{|s_2|}{\mu^2}\right)^{\omega_2}.$$

$$\left[1 + i\frac{\pi}{2} \left(\omega_1 + a \left(\ln \frac{\kappa_{12}}{\mu^2} - \frac{1}{\epsilon} \right) + \omega_3 + a \left(\ln \frac{\kappa_{23}}{\mu^2} - \frac{1}{\epsilon} \right) - i\pi a \left(\ln \frac{\kappa_{12} \kappa_{23}}{(\vec{q}_1 + \vec{q}_3 - \vec{q}_2)^2 q_2^2} \right) \right) \right]. \quad (120)$$

The square bracket expression is infrared finite. Comparison with (115) shows that the BDS formula correctly reproduces the one-loop approximation to $U_{\text{cut, reduced}}$, but not the higher order loops. Again, terms of order ϵ in $\ln M_{3 \rightarrow 3}$ cannot reproduce those finite (in ϵ) terms which are missing in M .

Discrepancies in the BDS finite pieces for six gluon amplitudes, starting at two loops, were also hinted in [46] where the equivalence between Wilson loops and MHV amplitudes was assumed. In a particular kinematic configuration, and for a very large number of external gluons at strong 't Hooft coupling, the finite pieces of the BDS ansatz failed when compared to the results of [47].

V. CONCLUSIONS

In this paper we have assembled the ingredients needed for the three-loop corrections (NNLO) to the BFKL kernel in $N = 4$ SYM theory at large N_c . Following earlier calculations we can obtain the kernel from unitarity sums, i.e. by computing squares of production amplitudes, keeping in mind that at large N_c the contributing diagrams belong to the cylinder topology. Figure 13 illustrates the production vertices which enter the three-loop calculation.

Elements in the first two lines are known, whereas the building blocks in the third line are new: they can be (and partly have been) computed from the effective action summarized in Sec. II.

For most of the cases, also the BDS formula can be used. The NNLO gluon trajectory function follows from the $2 \rightarrow 2$ scattering amplitude (first column); details are described in Appendix A. For the $2 \rightarrow 3$ case (second column), the two loop approximation to the gluon production vertex can be read off from the analysis presented in Sec. III (c.f. Eq. (49)). In this case one should take into account the ϵ -corrections to the BDS amplitude. In column 3, we should take into account the Reggeon + Reggeon $\rightarrow 2$ gluon vertex in the one-loop approximation for fixed invariant masses of produced gluons. Based upon the analysis carried out in Secs. III and IV we trust that the BDS formula for the maximal helicity violating case can be used (with ϵ -corrections). For the nonmaximal violating cases in column 3 one can use the results of [48]. Finally, in column 4 we encounter the Born vertex: Reggeon + Reggeon $\rightarrow 3$ gluons for the fixed invariant mass of the gluons. This vertex has been obtained in [30] by means of the effective action (see also Ref. [32]).

We have shown that the BDS amplitude $M_{2 \rightarrow 3}$ in the multi-Regge kinematics satisfies the dispersive representation, which is valid in all physical regions and is compatible with the Steinmann relations and gluon reggeization.

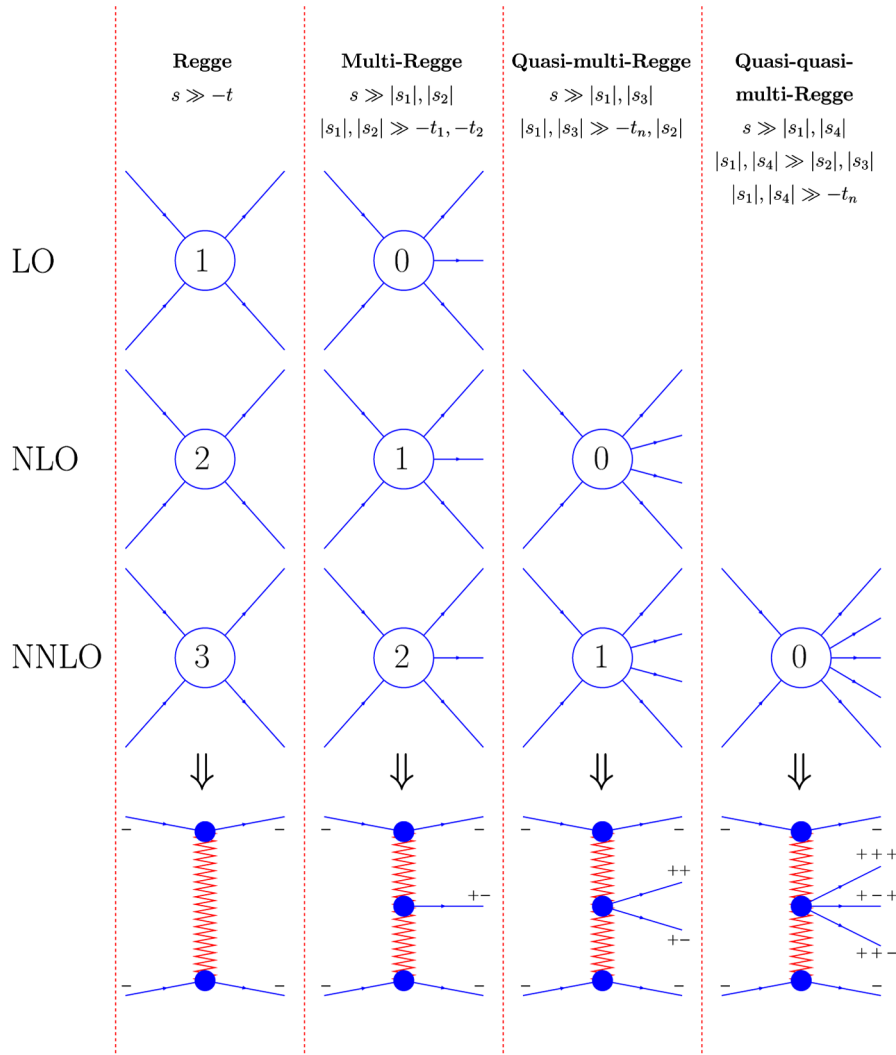


FIG. 13 (color online). Diagrams contributing to the BFKL kernel in NNLLA.

For the case of the gluon transitions $2 \rightarrow 4$ and $3 \rightarrow 3$, in the multi-Regge kinematics and in the physical region where $s, s_2 > 0$ and $s_1, s_3 < 0$, the Regge factorization of the BDS amplitude is badly violated. In the one-loop approximation the BDS result in this region coincides with the direct QCD calculations, but in higher loops we have shown that these amplitudes should contain the Mandelstam Regge cut in the t_2 -channel. It was demonstrated, that this cut is absent in the BDS expression and cannot be reproduced by the $\mathcal{O}(\epsilon)$ -corrections to this expression.

A remark is in place on the Regge cut contribution illustrated in Fig. 12 and discussed in Sec. IV. In addition to the corrections to the production vertex functions which are illustrated in Fig. 13, we still have to take into account those corrections to the production amplitude in the multi-Regge limit which do not fall into the class of loop corrections to the production vertices: in NLO these are just the Regge cut contributions to the imaginary part in the $2 \rightarrow 4$ and the $3 \rightarrow 3$ cases which we have discussed in the

previous section. The diagrams contributing to the BFKL Pomeron in the large N_c limit belong to the cylinder topology: two examples are illustrated in Fig. 14, and, to begin with, we consider the discontinuity due to the 4-particle intermediate state. In the left figure, on both sides of the discontinuity cut, we have the $3 \rightarrow 3$ production amplitudes continued into the physical region of a $2 \rightarrow 4$ process (cf. right-hand side of Fig. 12), and in the right-hand figure we recognize a configuration where the $2 \rightarrow 4$ amplitude has to be evaluated in a region with negative energies. As discussed before, in the latter case the non-factorizing pieces of the $2 \rightarrow 4$ production amplitude do not cancel. If these contributions would survive in the total cross section, the NNLO BFKL Pomeron would receive a four-Reggeon cut contribution, and the simple ladder structure would be lost. There are, however, reasons to expect that, in the large N_c limit, the sum of these contributions might cancel in the total cross section. Namely, in addition to the contribution of the 4-particle intermediate state, we also need other cuts, which, for example, run across one of

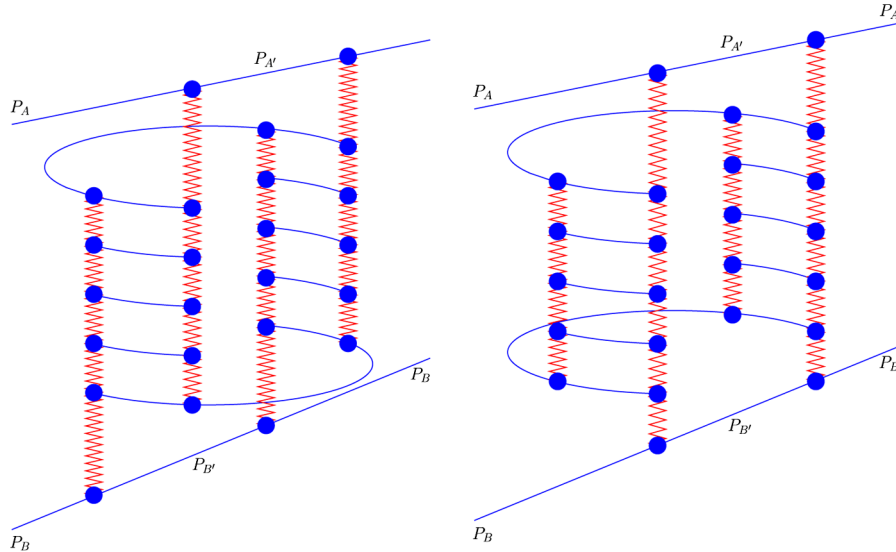


FIG. 14 (color online). Cylinder-type topologies in the unitarity sums for the total cross section: the intermediate states (discontinuity cuts) are obtained by slicing the cylinders in all possible ways across the intermediate momenta $p_{A'}$ and $p_{B'}$.

the ladders or along one of the reggeized gluons above or below the cylinder. These different cuts provide similar contributions, but they come with different signs. It is likely that, similar to the AFS cancellation of Regge cuts in planar amplitudes, the four Reggeon cut contributions cancel in the sum. We will study this in the subsequent part of our investigation.

During the refereeing process of this paper different interesting results have appeared in the literature related to our work. Among them we would like to mention the discovery of a dual superconformal symmetry of planar MHV scattering amplitudes in $N = 4$ SYM theory, which is an extension of the dual conformal symmetry, in [49,50]. This led to an interesting interpretation in terms of a fermionic T-duality of the connection between these amplitudes and Wilson loops in [51]. One of us found in [52] that in multi-Regge kinematics for certain physical regions where Mandelstam cuts appear, there exists a new integrable structure corresponding to an open spin chain. The connection between the dual superconformal symmetry and the integrability of the $AdS_5 \times S^5$ superstring was shown in [53]. A very interesting recent development was the formulation of functional equations defining the anomalous dimensions of the single trace operators in all orders of perturbation theory in the 't Hooft limit [54,55].

ACKNOWLEDGMENTS

We wish to thank V. S. Fadin, M. Strassler, and C. I. Tan for very helpful discussions. Part of this work has been done while one of us (A. S. V.) has been visiting the II. Institut f. Theoretische Physik, University Hamburg. The hospitality is gratefully acknowledged. One of us (L. N. L.) wishes to thank the Isaac Newton Institute for the invitation to participate in the program “String Fields, Integrability

and Strings.” L. N. L. is supported by the RFBR grants 06-02-72041-MNTI-a, 07-02-00902-a, and RSGSS-5788.2006.2.

Note added.—After our paper had been submitted, another study appeared which, in some parts, parallels our investigation [59]. Like ours, it studies several different Regge limits of the BDS amplitudes. In the unphysical region (negative energies), the results on the energy dependence are fully consistent with ours. In contrast to our paper, however, in [59] the continuation into physical regions has not been investigated, and the conflict with QCD calculations was not found. Recently another paper of these authors [60] has appeared which, in their versions 1 and 2, criticized our paper. We completely disagree with this criticism. More recently, a new version (version 3) appeared which strongly differs from the previous ones and does not contain the critical remarks of the first two versions. We still disagree with their statement in (4.20) for the 5-point function, implying that the Steinmann relations are violated in the BDS formula. In order to understand the Steinmann relations in massless gauge theories one can start, for example, with the Higgs mechanism for the gluon mass regularization (alternatively, one can also use a regularization scheme based upon Kaluza-Klein ideas, as explained in the second paper of [33]). In the Higgs model the gluon production vertex (the function G_2 in (4.11) of [60]) has two singularities in the κ -plane appearing at $\kappa_0 = 0$ and $\kappa_1 < 0$. Here the Steinmann relation can be established by the analytic continuation of the amplitude around the singularity at $\kappa_0 = 0$. In contrast, the continuation around the point κ_1 gives a nonphysical result for the discontinuities. In the massless limit, where $\kappa_1 \rightarrow 0$, the two cuts coincide and we lose the possibility to verify the Steinmann relation by the analytic continuation of M_5 to the correct second sheets. Nevertheless, the Steinmann

relation for two overlapping discontinuities, calculated with the use of the unitarity relations, continues to be valid in the massless limit contrary to the inequality (4.20) of [60]. Alternatively, one can verify the absence of the double discontinuities of the production amplitude $A_{2 \rightarrow 3}$ in the overlapping channels s_1 and s_2 (eq. (4.19) of [60]) for each individual Feynman diagram and for an arbitrary dimension $D = 4 - 2\epsilon$ of the space-time with the use of the energy-momentum conservation and the unitarity conditions in these channels (corresponding to the cuts similar to those appearing in the right-hand side of the diagrammatic equation Fig. 7 in [60]). In our paper we have verified explicitly that for the $n = 5$ BDS amplitude the analytic representation, (4.12) of [60], is compatible with the Steinmann relation and reproduces the scattering amplitude in all physical channels although, of course, it does not prove the validity of the BDS expression in this case. Therefore, we conclude that the analytic continuation chosen by the authors and leading to their expression (4.20) is not correct, even in the one-loop approximation. We want to stress that the violation of the Steinmann relation of the BDS amplitude for $n \geq 6$, which we discuss in our paper, is not due to the presence of massless particles, but due to an inconsistency of the BDS ansatz. In the case of massless theories, the analytic continuation of scattering amplitudes has to be done with care, and, when done correctly, it does not lead to a violation of the Steinmann relations.

The breakdown of the BDS ansatz for the 6-point amplitude in two loops demonstrated first in our paper was found by direct calculations [61] in agreement with the predictions from the Wilson-loop calculations [62].

Recently another paper on the high-energy behavior of the BDS formula appeared [63]. We do not agree with one of the main results, stating that in the multi-Regge kinematics the special functions appearing in the BDS ansatz are not important. To be more precise, the authors argue that the two limits: energy $s_2 \rightarrow \infty$ and $\epsilon \rightarrow 0$ do not commute. According to their appendix C, in the region $s, s_2 > 0, s_{345}, s_{456} < 0$ the sequence of limits: $\lim_{\epsilon \rightarrow 0} \lim_{s_2 \rightarrow \infty} F$ implies that the special functions do not contribute, whereas the opposite order $\lim_{s_2 \rightarrow \infty} \lim_{\epsilon \rightarrow 0} F$ leads to our result with the special functions being important. We disagree with this ‘‘noncommutativity,’’ since the first part of the authors’ argument is based on a simple arithmetic mistake. Namely, starting from Eq. (C.16), the multiplication of the factor $(-P^2)^{-\epsilon}$ with $(1 - \tilde{\Phi})^{-\epsilon}$ in Eq. (C.22), in the limit $s_2 \rightarrow \infty$, gives the *finite* expression $(p_{4\perp} + p_{5\perp})^{-2\epsilon}$, in agreement with Eq. (B.11). In this way the dependence on s_2 cancels out, both sequences of limits lead to the same answer (contrary to what is stated after Eq. (C.25)), and our result has been confirmed: in the BDS formula, the special functions are important in the multi-Regge kinematics, and their presence implies that the multi-Regge factorization is violated.

APPENDIX A: THE $2 \rightarrow 2$ AMPLITUDE

Let us write the BDS amplitude for the general case of n legs (see [31]):

$$\ln M_n = \sum_{l=1}^{\infty} a^l (f^{(l)}(\epsilon) (\hat{I}_n^{(1)}(l\epsilon) + F_n^{(1)}(0)) + C^{(l)} + E_n^{(l)}(\epsilon), \quad (\text{A1})$$

where $E_n^{(1)}(\epsilon)$ can be neglected for $\epsilon \rightarrow 0$, the values of the constants are

$$C^{(1)} = 0, \quad (\text{A2})$$

$$C^{(2)} = -\zeta_2^2/2, \quad (\text{A3})$$

$$f^{(l)}(\epsilon) = f_0^{(l)} + \epsilon f_1^{(l)} + \epsilon^2 f_2^{(l)}, \quad (\text{A4})$$

$$f_0^{(l)} = \frac{1}{4} \gamma_K^{(l)}, \quad (\text{A5})$$

$$f_1 = -a\zeta_3/2 + a^2(2\zeta_5 + 5\zeta_2\zeta_3/3), \quad (\text{A6})$$

γ_K is the cusp anomalous dimension [56],

$$\hat{I}_n^{(1)}(\epsilon) = -\frac{1}{2\epsilon^2} \sum_{i=1}^n \left(\frac{\mu^2}{-s_{i,i+1}} \right)^\epsilon, \quad (\text{A7})$$

and the finite remainders $F_n^{(1)}$ are expressed in terms of logarithms and dilogarithms. For the elastic scattering amplitude case we have

$$\hat{I}_4^{(1)}(\epsilon) = -\frac{2}{\epsilon^2} + \frac{1}{\epsilon} \ln \frac{(-s)(-t)}{\mu^4} - \frac{1}{2} \left(\ln^2 \frac{-s}{\mu^2} + \ln^2 \frac{-t}{\mu^2} \right), \quad (\text{A8})$$

$$F_4^{(1)} = -\frac{1}{2} \ln^2 \frac{-s}{-t} + 4\zeta_2. \quad (\text{A9})$$

Therefore

$$\hat{I}_4^{(1)}(\epsilon) + F_4^{(1)} = -\frac{2}{\epsilon^2} + \ln(-t) \frac{1}{\epsilon} + \ln(-s) \left(\frac{1}{\epsilon} - \ln \frac{-t}{\mu^2} \right) + 4\zeta_2. \quad (\text{A10})$$

As a result we obtain for M_4 Regge-type behavior, as already discussed in the main part of our paper, with the gluon Regge trajectory given by

$$\omega(t) = a \left(\frac{1}{\epsilon} - \ln \frac{-t}{\mu^2} \right) + a^2 \left(-\zeta_2 \left(\frac{1}{2\epsilon} - \ln \frac{-t}{\mu^2} \right) - \frac{\zeta_3}{2} \right) + \dots \quad (\text{A11})$$

Note that this result at two loops is in agreement with the

direct calculations [2,3] based on the BFKL approach [1]. Indeed, in Ref. [3] the following expression for the gluon Regge trajectory was obtained in the $\overline{\text{MS}}$ -scheme (using the same notations):

$$\omega_{\overline{\text{MS}}}(t) = a \left(\frac{1}{\epsilon} - \ln \frac{-t}{\mu^2} \right) + a^2 \left[\left(\frac{1}{6} - \zeta_2 \right) \left(\frac{1}{2\epsilon} - \ln \frac{-t}{\mu^2} \right) + \frac{2}{9} - \frac{\zeta_3}{2} \right]. \quad (\text{A12})$$

The contribution of the scalar loop to this trajectory is proportional to the contribution of the fermion loop [3]

$$\begin{aligned} \omega_{\overline{\text{MS}}}^s(t) &= \frac{n_s}{4n_q} \frac{1}{1-\epsilon} \omega_{\overline{\text{MS}}}^q(t) \\ &= n_s \frac{a^2}{24} \left[\frac{1}{\epsilon^2} - \ln \frac{-t}{\mu^2} - \frac{8}{3} \left(\frac{1}{\epsilon} + 2 \ln \frac{-t}{\mu^2} \right) - \frac{52}{9} \right], \end{aligned} \quad (\text{A13})$$

where n_s is the number of scalar fields transforming according to the adjoint representation of the gauge group. For the transition from the $\overline{\text{MS}}$ -scheme to the dimensional reduction (DRED) scheme, which respects $N = 4$ supersymmetry, one should first increase the number of scalar fields

$$n_s \rightarrow 6 + 2\epsilon, \quad (\text{A14})$$

because, in the pure gluonic contribution, $\Delta n = -2\epsilon$ for the gluon fields was taken into account after performing the dimensional regularization $4 \rightarrow 4 - 2\epsilon$. This gives the additional contribution to $\omega_{\overline{\text{MS}}}(t)$

$$\Delta \omega_{\overline{\text{MS}}}(t) = \frac{a^2}{12} \left(\frac{1}{\epsilon} - \frac{8}{3} \right). \quad (\text{A15})$$

After that the subsequent finite renormalization of the coupling constant needed for the transition between the $\overline{\text{MS}}$ and DRED schemes

$$a \rightarrow a - \frac{1}{6} a^2 \quad (\text{A16})$$

leads to the above result for the trajectory

$$\begin{aligned} \omega_{\overline{\text{MS}}}(t) &\rightarrow \omega(t) \\ &= a \left(\frac{1}{\epsilon} - \ln \frac{-t}{\mu^2} \right) + a^2 \left[-\zeta_2 \left(\frac{1}{2\epsilon} - \ln \frac{-t}{\mu^2} \right) - \frac{\zeta_3}{2} \right]. \end{aligned} \quad (\text{A17})$$

Concerning the residues $\Gamma(t)$ of the Regge pole, they have been calculated in the one-loop approximation in QCD [33]. In supersymmetric models the helicity non-conserving contribution of each of the colliding gluons is cancelled, in accordance with the BDS ansatz.

APPENDIX B: THE $2 \rightarrow 3$ AMPLITUDE

For the $2 \rightarrow 3$ production amplitude we have (see Fig. 3)

$$\begin{aligned} \hat{I}_5^{(1)}(\epsilon) &= -\frac{5}{2\epsilon^2} + \frac{1}{2\epsilon} \ln \frac{(-s)(-s_1)(-s_2)(-t_1)(-t_2)}{\mu^{10}} \\ &\quad - \frac{1}{4} \left(\ln^2 \frac{-s}{\mu^2} + \ln^2 \frac{-s_1}{\mu^2} + \ln^2 \frac{-s_2}{\mu^2} + \ln^2 \frac{-t_1}{\mu^2} \right. \\ &\quad \left. + \ln^2 \frac{-t_2}{\mu^2} \right), \end{aligned} \quad (\text{B1})$$

$$\begin{aligned} F_5^{(1)} &= -\frac{1}{4} \ln \frac{-s}{-s_1} \ln \frac{-t_2}{-s_2} - \frac{1}{4} \ln \frac{-t_2}{-t_1} \ln \frac{-s_2}{-s_1} \\ &\quad - \frac{1}{4} \ln \frac{-s_2}{-s} \ln \frac{-s_1}{-t_1} - \frac{1}{4} \ln \frac{-s_1}{-t_2} \ln \frac{-t_1}{-s} \\ &\quad - \frac{1}{4} \ln \frac{-t_1}{-s_2} \ln \frac{-s}{-t_2} + \frac{15}{4} \zeta_2. \end{aligned} \quad (\text{B2})$$

Thus the total contribution in multi-Regge kinematics is

$$\begin{aligned} I_5^{(1)}(\epsilon) + F_5^{(1)} &= -\frac{5}{2\epsilon^2} + \ln \frac{-s_1}{\mu^2} \left(\frac{1}{\epsilon} - \ln \frac{-t_1}{\mu^2} \right) \\ &\quad + \ln \frac{-s_2}{\mu^2} \left(\frac{1}{\epsilon} - \ln \frac{-t_2}{\mu^2} \right) + \frac{1}{2\epsilon} \ln \frac{(-t_1)(-t_2)}{\mu^4} \\ &\quad - \frac{1}{4} \ln^2 \frac{-\kappa}{\mu^2} + \frac{1}{2} \ln \frac{-\kappa}{\mu^2} \left(\ln \frac{(-t_1)(-t_2)}{\mu^4} - \frac{1}{\epsilon} \right) \\ &\quad - \frac{1}{4} \ln^2 \frac{-t_1}{-t_2} + \frac{15}{4} \zeta_2. \end{aligned} \quad (\text{B3})$$

In this way we obtain the Regge factorization of the production amplitudes, discussed in the main text. Let us note that, formally, this result is exact and the amplitude can be written in this factorized form in all five channels obtained by the cyclic transmutation of the invariants s, t_1, s_1, s_2, t_2 .

In the one-loop approximation in QCD the Reggeon-Reggeon-gluon vertex contains, apart from the Born structure proportional to the vector $C(q_2, q_1)$, also the contribution proportional to the gauge-invariant vector $\frac{p_A}{s_1} - \frac{p_B}{s_2}$ [33]. In the supersymmetric theories this contribution is cancelled, in agreement with the BDS ansatz.

One can calculate also the production amplitude in the quasielastic kinematics, where $s \sim s_1 \gg s_2 \sim t_1, t_2, k_{\perp}^2$. The amplitude here has the usual Regge factorization.

APPENDIX C: THE $2 \rightarrow 4$ AMPLITUDE

In the case of the $2 \rightarrow 4$ transition we have (see Fig. 6)

$$\begin{aligned} \hat{I}_6^{(1)}(\epsilon) &= -\frac{3}{\epsilon^2} + \frac{1}{2\epsilon} \ln \frac{(-s)(-s_1)(-s_2)(-s_3)(-t_1)(-t_3)}{\mu^{12}} \\ &\quad - \frac{1}{4} \left(\ln^2 \frac{-s}{\mu^2} + \ln^2 \frac{-s_1}{\mu^2} + \ln^2 \frac{-s_2}{\mu^2} \right. \\ &\quad \left. + \ln^2 \frac{-s_3}{\mu^2} + \ln^2 \frac{-t_1}{\mu^2} + \ln^2 \frac{-t_3}{\mu^2} \right), \end{aligned} \quad (\text{C1})$$

$$\begin{aligned}
 F_6^{(1)} = & -\frac{1}{2} \ln \frac{-s}{-s_{012}} \ln \frac{-t_3}{-s_{012}} - \frac{1}{2} \ln \frac{-t_3}{-t_2} \ln \frac{-s_3}{-t_2} - \frac{1}{2} \ln \frac{-s_3}{-s_{123}} \ln \frac{-s_2}{-s_{123}} - \frac{1}{2} \ln \frac{-s_2}{-s_{012}} \ln \frac{-s_1}{-s_{012}} - \frac{1}{2} \ln \frac{-s_1}{-t_2} \ln \frac{-t_1}{-t_2} \\
 & - \frac{1}{2} \ln \frac{-t_1}{-s_{123}} \ln \frac{-s}{-s_{123}} - \frac{1}{2} \text{Li}_2 \left(1 - \frac{s s_2}{s_{012} s_{123}} \right) - \frac{1}{2} \text{Li}_2 \left(1 - \frac{t_3 s_1}{t_2 s_{012}} \right) - \frac{1}{2} \text{Li}_2 \left(1 - \frac{t_1 s_3}{t_2 s_{123}} \right) + \frac{1}{4} \left(\ln \frac{-t_2}{-s_{012}} \right)^2 \\
 & + \frac{1}{4} \left(\ln \frac{-t_2}{-s_{123}} \right)^2 + \frac{1}{4} \left(\ln \frac{-s_{123}}{-s_{012}} \right)^2 + \frac{9}{2} \zeta_2,
 \end{aligned} \tag{C2}$$

where the dilogarithm function is defined as

$$\text{Li}_2(z) = - \int_0^z \frac{dt}{t} \ln(1-t). \tag{C3}$$

In multi-Regge kinematics it is natural to introduce the independent variables

$$s_1, s_2, s_3, -\kappa_{12} = \frac{(-s_1)(-s_2)}{(-s_{012})}, \quad -\kappa_{23} = \frac{(-s_2)(-s_3)}{(-s_{123})}, \quad \Phi = \frac{(-s)(-s_2)}{(-s_{012})(-s_{123})}. \tag{C4}$$

Note that the variable Φ is unity in the region where all above invariants are negative, but $\Phi = \exp(-2\pi i)$ in the physical region where $s, s_2 > 0, s_{012}, s_{123} < 0$. In the multi-Regge kinematics we obtain the following general result:

$$\begin{aligned}
 I_6^{(1)}(\epsilon) + F_6^{(1)} = & -\frac{3}{\epsilon^2} - \frac{1}{4} \ln^2 \Phi - \frac{1}{2} \ln \Phi \left(\ln \frac{(-t_1)(-t_3)}{(-s_2)\mu^2} - \frac{1}{\epsilon} \right) - \frac{1}{2} \text{Li}_2(1-\Phi) + \ln \frac{-s_1}{\mu^2} \left(\frac{1}{\epsilon} - \ln \frac{-t_1}{\mu^2} \right) \\
 & + \ln \frac{-s_2}{\mu^2} \left(\frac{1}{\epsilon} - \ln \frac{-t_2}{\mu^2} \right) + \ln \frac{-s_3}{\mu^2} \left(\frac{1}{\epsilon} - \ln \frac{-t_3}{\mu^2} \right) - \frac{1}{4} \left(\ln^2 \frac{-\kappa_{12}}{\mu^2} + \ln^2 \frac{-\kappa_{23}}{\mu^2} \right) \\
 & + \frac{1}{2} \ln \frac{-\kappa_{12}}{\mu^2} \left(\ln \frac{(-t_1)(-t_2)}{\mu^4} - \frac{1}{\epsilon} \right) + \frac{1}{2\epsilon} \ln \frac{(-t_1)(-t_3)}{\mu^4} + \frac{1}{2} \ln \frac{-\kappa_{23}}{\mu^2} \left(\ln \frac{(-t_2)(-t_3)}{\mu^4} - \frac{1}{\epsilon} \right) \\
 & - \frac{1}{4} \left(\ln^2 \frac{-t_1}{-t_2} + \ln^2 \frac{-t_3}{-t_2} \right) + \frac{7}{2} \zeta_2.
 \end{aligned} \tag{C5}$$

At first sight the arguments of the dilogarithm functions in the multi-Regge kinematics are either 0 or 1, and we can use the relations

$$\text{Li}_2(0) = 0, \quad \text{Li}_2(1) = \zeta_2. \tag{C6}$$

However, in the physical region $s, s_2 > 0, s_1, s_3, s_{012}, s_{123} < 0$ it is needed to be cautious: we should analytically continue the expression

$$f(\Phi) = \text{Li}_2(1-\Phi), \quad \Phi = \frac{s s_2}{s_{012} s_{123}} \tag{C7}$$

from the region $\Phi \approx 1$ to the region $\Phi \approx e^{-2\pi i}$ along a unit circle. In multi-Regge kinematics we have

$$s_2 \approx \frac{s_{012} s_{123}}{s} - (\vec{k}_1 + \vec{k}_2)^2 \tag{C8}$$

and

$$s_2(1-\Phi)\Phi^{-1} = (\vec{k}_1 + \vec{k}_2)^2. \tag{C9}$$

Therefore $1-\Phi > 0$, and after the analytic continuation we obtain

$$\begin{aligned}
 f(\Phi) = & - \int_0^{1-\Phi} \frac{dt}{t} \ln(1-t) + 2\pi i \int_1^{1-\Phi} \frac{dt}{t} \\
 \approx & 2\pi i \ln(1-\Phi)
 \end{aligned} \tag{C10}$$

with $\ln(1-\Phi)$ being real valued. We obtain the following result in the physical region $s, s_2 > 0, s_1, s_3, s_{012}, s_{123} < 0$:

$$\begin{aligned}
 I_6^{(1)}(\epsilon) + F_6^{(1)} = & -\frac{3}{\epsilon^2} + \pi i \left(\ln \frac{(-t_1)(-t_3)}{(\vec{k}_1 + \vec{k}_2)^2 \mu^2} - \frac{1}{\epsilon} \right) + \ln \frac{-s_1}{\mu^2} \left(\frac{1}{\epsilon} - \ln \frac{-t_1}{\mu^2} \right) + \ln \frac{-s_2}{\mu^2} \left(\frac{1}{\epsilon} - \ln \frac{-t_2}{\mu^2} \right) + \ln \frac{-s_3}{\mu^2} \left(\frac{1}{\epsilon} - \ln \frac{-t_3}{\mu^2} \right) \\
 & - \frac{1}{4} \left(\ln^2 \frac{-\kappa_{12}}{\mu^2} + \ln^2 \frac{-\kappa_{23}}{\mu^2} \right) + \frac{1}{2} \ln \frac{-\kappa_{12}}{\mu^2} \left(\ln \frac{-t_1}{\mu^2} + \ln \frac{-t_2}{\mu^2} - \frac{1}{\epsilon} \right) + \frac{1}{2} \ln \frac{-\kappa_{23}}{\mu^2} \left(\ln \frac{-t_2}{\mu^2} + \ln \frac{-t_3}{\mu^2} - \frac{1}{\epsilon} \right) \\
 & - \frac{1}{4} \left(\ln^2 \frac{-t_1}{-t_2} + \ln^2 \frac{-t_3}{-t_2} \right) + \frac{1}{2\epsilon} \ln \frac{(-t_1)(-t_3)}{\mu^4} + \frac{7}{2} \zeta_2.
 \end{aligned} \tag{C11}$$

It is possible to derive, from the BDS amplitude, an expression for $M_{2 \rightarrow 4}$ in the one-loop approximation for the quasi-multi-Regge kinematics, where $s \gg s_1, s_3 \gg s_2 \sim t_1, t_2, t_3$. In this case it is convenient to introduce Sudakov variables for the momenta of the two produced particles

$$k_r = \beta_r p_A + \alpha_r p_B + k_r^\perp, \quad (k_r^\perp)^2 = -\vec{k}_r^2, \quad (\text{C12})$$

where

$$1 \gg \beta_1 \sim \beta_2 \gg \frac{\mu^2}{s}, \quad 1 \gg \alpha_1 \sim \alpha_2 \gg \frac{\mu^2}{s}, \quad (\text{C13})$$

$$s\alpha_r\beta_r = \vec{k}_r^2 \sim \vec{q}_1^2 \sim \vec{q}_2^2 \sim \vec{q}_3^2 \sim \mu^2.$$

We can express various invariants in terms of these variables

$$\begin{aligned} \Delta f = & -\frac{1}{2} \ln \frac{s\kappa_{12}\kappa_{23}}{s_1s_2s_3} \ln \frac{st_1t_3}{s_{012}s_{123}\mu^2} + \frac{1}{2} \ln \frac{s_{012}\kappa_{12}}{s_1s_2} \ln \frac{t_3s_1s_2s}{t_2s_{012}^2s_{123}} + \frac{1}{2} \ln \frac{s_{123}\kappa_{23}}{s_3s_2} \ln \frac{t_1s_3s_2s}{t_2s_{012}s_{123}^2} - \frac{1}{4} \ln^2 \frac{s\kappa_{12}\kappa_{23}}{s_1s_2s_3} - \frac{1}{2} \ln^2 \frac{s_{012}\kappa_{12}}{s_1s_2} \\ & - \frac{1}{2} \ln^2 \frac{s_{123}\kappa_{23}}{s_3s_2} - \frac{1}{2} \ln \frac{s\kappa_{12}\kappa_{23}}{s_1s_2s_3} \ln \frac{s_{012}s_{123}\kappa_{12}\kappa_{23}}{s_1s_3s_2^2} - \frac{1}{2} \ln \frac{s_{012}\kappa_{12}}{s_1s_2} \ln \frac{s_{123}\kappa_{23}}{s_3s_2} + \zeta_2 - \frac{1}{2} \text{Li}_2\left(1 - \frac{ss_2}{s_{012}s_{123}}\right) \\ & - \frac{1}{2} \text{Li}_2\left(1 - \frac{t_3s_1}{t_2s_{012}}\right) - \frac{1}{2} \text{Li}_2\left(1 - \frac{t_1s_3}{t_2s_{123}}\right). \end{aligned} \quad (\text{C17})$$

Here the signs -1 are implied to be in front of all invariants s_i, t_i . Note that the expression for Δf in the quasi-multi-Regge kinematics does not contain large logarithms, because the arguments of all logarithms and dilogarithm functions are of the order of unity. It is proportional to the logarithm of the amplitude for the transition of two Reggeized gluons into two particles with the same helicity. Similar to the case of M_4 and M_5 the expression for $M_{2 \rightarrow 4}$ in the quasi-multi-Regge kinematics coincides with the exact BDS amplitude. The transition of two Reggeons to particles with opposite helicity in the one-loop approximation can be found in Ref. [48]. These transition amplitudes are needed for the calculation of the next-to-next-to leading corrections to the BFKL equation.

APPENDIX D: THE $3 \rightarrow 3$ AMPLITUDE

Here we consider the BDS amplitude M_6 in the channel corresponding to the transition $3 \rightarrow 3$ with the following

bles

$$s_2 \approx s(\beta_1 + \beta_2)(\alpha_1 + \beta_2) - (\vec{k}_1 + \vec{k}_2)^2, \quad (\text{C14})$$

$$s_1 \approx \alpha_1 s, \quad s_3 \approx \beta_2 s, \quad s_{012} \approx (\alpha_1 + \alpha_2)s, \quad (\text{C15})$$

$$s_{123} \approx (\beta_1 + \beta_2)s.$$

The expression for the function $f(\epsilon) = I_6^{(1)}(\epsilon) + F_6^{(1)}$ (for $\Phi = 1$) in the quasi-multi-Regge kinematics can be obtained by adding an additional term

$$f(\epsilon) \rightarrow f(\epsilon) + \Delta f, \quad (\text{C16})$$

where

invariants (see Fig. 9):

$$s = (p_A + k_1 + p_B)^2, \quad s_1 = (p_A + k_1)^2, \quad (\text{D1})$$

$$s_3 = (p_{B'} + k_2)^2,$$

$$s_{13} = (k_1 + p_B)^2, \quad s_{02} = (p_{A'} + k_2)^2, \quad (\text{D2})$$

$$t'_2 = (p_{A'} + k_2 - p_A)^2,$$

$$t_1 = (p_{A'} - p_A)^2, \quad t_3 = (p_{B'} - p_B)^2, \quad (\text{D3})$$

$$t_2 = (p_{A'} - p_A - k_1)^2.$$

The functions $\hat{I}_6^{(1)}(\epsilon)$ and $F_6^{(1)}$ in this case are given by [31]:

$$\begin{aligned} \hat{I}_6^{(1)}(\epsilon) = & -\frac{3}{\epsilon^2} + \frac{1}{2\epsilon} \ln \frac{(-s_1)(-s_{13})(-s_3)(-s_{02})(-t_1)(-t_3)}{\mu^{12}} \\ & - \frac{1}{4} \left(\ln^2 \frac{-s_1}{\mu^2} + \ln^2 \frac{-s_{13}}{\mu^2} + \ln^2 \frac{-s_3}{\mu^2} + \ln^2 \frac{-s_{02}}{\mu^2} + \ln^2 \frac{-t_1}{\mu^2} + \ln^2 \frac{-t_3}{\mu^2} \right), \end{aligned} \quad (\text{D4})$$

$$\begin{aligned}
F_6^{(1)} = & -\frac{1}{2} \ln \frac{-s_1}{-s} \ln \frac{-s_{13}}{-s} - \frac{1}{2} \ln \frac{-s_{13}}{-t'_2} \ln \frac{-t_3}{-t'_2} - \frac{1}{2} \ln \frac{-t_3}{-t_2} \ln \frac{-s_3}{-t_2} - \frac{1}{2} \ln \frac{-s_3}{-s} \ln \frac{-s_{02}}{-s} - \frac{1}{2} \ln \frac{-s_{02}}{-t'_2} \ln \frac{-t_1}{-t'_2} - \frac{1}{2} \ln \frac{-t_1}{-t_2} \ln \frac{-s_1}{-t_2} \\
& - \frac{1}{2} \text{Li}_2 \left(1 - \frac{s_1 s_3}{s t_2} \right) - \frac{1}{2} \text{Li}_2 \left(1 - \frac{s_{13} s_{02}}{t'_2 s} \right) - \frac{1}{2} \text{Li}_2 \left(1 - \frac{t_1 t_3}{t'_2 t_2} \right) + \frac{1}{4} \left(\ln \frac{-t'_2}{-s} \right)^2 + \frac{1}{4} \left(\ln \frac{-t'_2}{-t_2} \right)^2 + \frac{1}{4} \left(\ln \frac{-t_2}{-s} \right)^2 + \frac{9}{2} \zeta_2.
\end{aligned} \tag{D5}$$

In multi-Regge kinematics

$$-s \gg -s_1, -s_3, -t'_2 \gg -t_1, -t_2, -t_3 > 0 \tag{D6}$$

it is helpful to use the definitions

$$-\kappa_{12} = \frac{(-s_1)(-t'_2)}{-s_{02}}, \quad -\kappa_{23} = \frac{(-s_3)(-t'_2)}{-s_{13}}, \quad \Phi' = \frac{(-s_{13})(-s_{02})}{(-t'_2)(-s)}, \tag{D7}$$

which allows us to simplify the above expressions

$$\begin{aligned}
I_6^{(1)}(\epsilon) + F_6^{(1)} = & -\frac{3}{\epsilon^2} - \frac{1}{2} \ln^2 \Phi' - \frac{1}{2} \ln \Phi' \ln \frac{(-\kappa_{12})(-\kappa_{23})}{(-t'_2)(-t_2)} - \frac{1}{2} \text{Li}_2(1 - \Phi') + \ln \frac{-s_1}{\mu^2} \left(\frac{1}{\epsilon} - \ln \frac{-t_1}{\mu^2} \right) + \ln \frac{-t'_2}{\mu^2} \left(\frac{1}{\epsilon} - \ln \frac{-t_2}{\mu^2} \right) \\
& + \ln \frac{-s_3}{\mu^2} \left(\frac{1}{\epsilon} - \ln \frac{-t_3}{\mu^2} \right) - \frac{1}{4} \left(\ln^2 \frac{-\kappa_{12}}{\mu^2} + \ln^2 \frac{-\kappa_{23}}{\mu^2} \right) + \frac{1}{2} \ln \frac{-\kappa_{12}}{\mu^2} \left(\ln \frac{(-t_1)(-t_2)}{\mu^4} - \frac{1}{\epsilon} \right) + \frac{1}{2\epsilon} \ln \frac{(-t_1)(-t_3)}{\mu^4} \\
& + \frac{1}{2} \ln \frac{-\kappa_{23}}{\mu^2} \left(\ln \frac{(-t_2)(-t_3)}{\mu^4} - \frac{1}{\epsilon} \right) - \frac{1}{4} \left(\ln^2 \frac{-t_1}{-t_2} + \ln^2 \frac{-t_3}{-t_2} \right) + \frac{7}{2} \zeta_2.
\end{aligned} \tag{D8}$$

In the physical region, where $s, t'_2 > 0$ and $s_1, s_3, s_{02}, s_{13} < 0$, one has $\Phi' = \exp(2\pi i)$, i.e. we have to continue in Φ' along the unit circle. The relation

$$-t'_2(1 - \Phi') \approx (\vec{q}_1 + \vec{q}_3 - \vec{q}_2)^2 \tag{D9}$$

implies that, after continuation, $1 - \Phi' < 0$. Therefore, Li_2 becomes

$$\begin{aligned}
f(\Phi') = & -\int_0^{1-\Phi'} \frac{dt}{t} \ln(1-t) - 2\pi i \int_1^{1-\Phi'} \frac{dt}{t} \\
\approx & 2\pi^2 - 2\pi i \ln|1 - \Phi'|,
\end{aligned} \tag{D10}$$

which allows to obtain the extra phase factor C' violating the Regge factorization in this physical region.

APPENDIX E: HIGH ENERGY SCATTERING AMPLITUDES IN THE LEADING LOGARITHMIC APPROXIMATION

In this appendix we briefly summarize results for the high-energy $2 \rightarrow 3$, $2 \rightarrow 4$, and $3 \rightarrow 3$ scattering amplitudes in Yang-Mills theories in the leading logarithmic approximation.

For the $2 \rightarrow 3$ case most of the results have already been listed in Sec. IV B. We only quote, for the physical region where all energies are positive, the factorized form:

$$\frac{A_{2 \rightarrow 3}}{\Gamma(t_1)\Gamma(t_2)} = \frac{2s}{t_1 t_2}.$$

$$(e^{-i\pi}|s_1|)^{\omega_1} \frac{(e^{-i\pi}\kappa_{12})^{-\omega_2} V_1(t_1, t_2, \kappa_{12}) - (e^{-i\pi}\kappa_{12})^{-\omega_1} V_2(t_1, t_2, \kappa_{12})}{\sin\pi(\omega_1 - \omega_2)} (e^{-i\pi}|s_2|)^{\omega_2}. \tag{E1}$$

Here the trajectory functions ω_i and the production vertices V_1, V_2 have been computed in LLA and NLO, whereas the phases and sin factors are part of the analytic representation, and do not need to be expanded in powers of g^2 . However, since in this paper we restrict ourselves to the LLA, we can put $(e^{-i\pi}\kappa_{12})^{-\omega_1} \approx 1$. For the real part we find the result (96) which coincides with (4).

For the $2 \rightarrow 4$ amplitude we start from the ansatz (97):

$$\begin{aligned}
 \frac{A_{2 \rightarrow 4}}{\Gamma(t_1)\Gamma(t_3)} &= \frac{2s}{t_1 t_2 t_3} \int \frac{d\omega'_2}{2\pi i} \left[\left(\frac{|s_1|}{\mu^2} \right)^{\omega_1 - \omega'_2} \left(\frac{|s_{012}|}{\mu^2} \right)^{\omega'_2 - \omega_3} \left(\frac{|s|}{\mu^2} \right)^{\omega_3} \xi_{12'} \xi_{2'3} \xi_3 \frac{W_1(t_1, t_2, t_3, \kappa_{12}, \kappa_{23}; \omega'_2)}{\sin \pi \omega_{12'} \sin \pi \omega_{2'3}} \right. \\
 &+ \left(\frac{|s_3|}{\mu^2} \right)^{\omega_3 - \omega'_2} \left(\frac{|s_{123}|}{\mu^2} \right)^{\omega'_2 - \omega_1} \left(\frac{|s|}{\mu^2} \right)^{\omega_1} \xi_{32'} \xi_{2'1} \xi_1 \frac{W_2(t_1, t_2, t_3, \kappa_{12}, \kappa_{23}; \omega'_2)}{\sin \pi \omega_{32'} \sin \pi \omega_{2'1}} \\
 &+ \left(\frac{|s_2|}{\mu^2} \right)^{\omega'_2 - \omega_1} \left(\frac{|s_{012}|}{\mu^2} \right)^{\omega_1 - \omega_3} \left(\frac{|s|}{\mu^2} \right)^{\omega_3} \xi_{2'1} \xi_{13} \xi_3 \frac{W_3(t_1, t_2, t_3, \kappa_{12}, \kappa_{23}, \kappa_{123}; \omega'_2)}{\sin \pi \omega_{2'1} \sin \pi \omega_{13}} \\
 &+ \left(\frac{|s_2|}{\mu^2} \right)^{\omega'_2 - \omega_3} \left(\frac{|s_{123}|}{\mu^2} \right)^{\omega_3 - \omega_1} \left(\frac{|s|}{\mu^2} \right)^{\omega_1} \xi_{2'3} \xi_{31} \xi_1 \frac{W_4(t_1, t_2, t_3, \kappa_{12}, \kappa_{23}, \kappa_{123}; \omega'_2)}{\sin \pi \omega_{2'3} \sin \pi \omega_{31}} \\
 &\left. + \left(\frac{|s_3|}{\mu^2} \right)^{\omega_3 - \omega'_2} \left(\frac{|s_1|}{\mu^2} \right)^{\omega_1 - \omega'_2} \left(\frac{|s|}{\mu^2} \right)^{\omega_2} \xi_{32'} \xi_{12'} \xi_{2'} \frac{W_5(t_1, t_2, t_3, \kappa_{12}, \kappa_{23}; \omega'_2)}{\sin \pi \omega_{32'} \sin \pi \omega_{12'}} \right]. \tag{E2}
 \end{aligned}$$

The partial wave functions $W_{i=1,2,3,4,5}$ have been listed in Sec. IV B. They have been obtained from the five single energy discontinuity equations, and use has been made of the BFKL bootstrap equations in the color octet channel.

Inserting these partial waves into the ansatz (97) or (E2), we can study the full amplitude in the different kinematic regions. From now on we will specialize on the planar approximation, i.e. in the signature factors in Eq. (93) we only retain the phases.

Beginning with the physical region where all energies are positive, we first collect the Regge pole terms in all five partial waves W_i . Their sum can be written in the simple factorizing form:

$$\begin{aligned}
 \frac{A_{2 \rightarrow 4, \text{pole}}}{\Gamma(t_1)\Gamma(t_3)} &= \frac{2s}{t_1 t_2 t_3} \cdot \frac{(e^{-i\pi|s_1|})^{\omega_2} (e^{-i\pi\kappa_{12}})^{-\omega_2} V_1(t_1, t_2, \kappa_{12}) - (e^{-i\pi\kappa_{12}})^{-\omega_1} V_2(t_1, t_2, \kappa_{12})}{\sin \pi \omega_{12}} (e^{-i\pi|s_2|})^{\omega_2} \\
 &\cdot \frac{(e^{-i\pi\kappa_{23}})^{-\omega_3} V_1(t_2, t_3, \kappa_{23}) - (e^{-i\pi\kappa_{23}})^{-\omega_2} V_2(t_2, t_3, \kappa_{23})}{\sin \pi \omega_{23}} (e^{-i\pi|s_3|})^{\omega_3}. \tag{E3}
 \end{aligned}$$

In order to arrive at this result, we have combined, in (100) and (101), the Regge pole contributions of W_3 and W_4 (together with the signature factors), and we have used the identity:

$$\frac{\sin \pi \omega_{23}}{\sin \pi \omega_{13}} \cdot \frac{\sin \pi \omega_1}{\sin \pi \omega_2} + \frac{\sin \pi \omega_{21}}{\sin \pi \omega_{31}} \cdot \frac{\sin \pi \omega_3}{\sin \pi \omega_2} = 1. \tag{E4}$$

The production vertices are the same as in the $2 \rightarrow 3$ case, (E1). As in the $2 \rightarrow 3$ case, in the leading order approximation we put, in (E3), $(e^{-i\pi\kappa})^{-\omega} \approx 1$. For the real part the terms proportional to $\ln(\kappa/\mu^2) - \frac{1}{\epsilon}$ in the production vertices V_1 and V_2 cancel, and we are back to the factorizing form in (4). As to the additional Regge cut pieces contained in W_3 and W_4 , they cancel completely:

$$\begin{aligned}
 \frac{A_{2 \rightarrow 4, \text{cut}}}{\Gamma(t_1)\Gamma(t_3)} &= \frac{-2s}{t_1 t_2 t_3} \cdot (|s_1|)^{\omega_1} \int \frac{d\omega'_2}{2\pi i} (e^{-i\pi|s_2|})^{\omega'_2} \\
 &\times \left(\frac{1}{\sin \pi \omega_{13}} + \frac{1}{\sin \pi \omega_{31}} \right) (V_{\text{cut}} - V_p) (|s_3|)^{\omega_3} \\
 &= 0. \tag{E5}
 \end{aligned}$$

It is instructive to study the cancellation of the imaginary

part of this Regge cut piece in more detail: from the representation (97) which shows the energy phase factors explicitly it is straightforward to compute the single discontinuities in s_2, s_{012}, s_{123} , and in s . When summing these single discontinuities (i.e. when computing the full imaginary part), we find complete cancellation of the Regge cut piece. This cancellation of Regge cut contributions in the planar amplitude is nothing else but the Mandelstam mechanism [57] of the cancellation of the Amati-Fubini-Stanghellini Regge cut [58] in planar diagrams.

The unphysical region where all energies are negative can be obtained from (E3) and (E5) by simply putting the phase factors equal to unity: the factorizing form of the Regge-pole contributions is preserved, and the cut pieces in W_3 and W_4 cancel.

Most interesting is the physical region where $s, s_2 > 0$ and $s_1, s_3, s_{012}, s_{123} < 0$. Nonzero phases appear only in s and in s_2 . After some algebra we rewrite (E2) in the following form:

$$\frac{A_{2 \rightarrow 4}}{\Gamma(t_1)\Gamma(t_3)} = \frac{2s}{t_1 t_2 t_3} (|s_1|)^{\omega_1} (|s_3|)^{\omega_3}. \tag{E6}$$

$$\begin{aligned}
& e^{-i\pi\omega_2}(|s_2|)^{\omega_2} \left[\left(\frac{V_1}{\sin\pi\omega_{12}} + e^{-i\pi\omega_{12}} \frac{V_2}{\sin\pi\omega_{21}} \right) \left(e^{-i\pi\omega_{32}} \frac{V_1}{\sin\pi\omega_{23}} + \frac{V_1}{\sin\pi\omega_{32}} \right) \right. \\
& \times \left(e^{-i\pi\omega_{31}} \frac{\sin\pi\omega_1 \sin\pi\omega_{23}}{\sin\pi\omega_2 \sin\pi\omega_{13}} + e^{-i\pi\omega_{13}} \frac{\sin\pi\omega_3 \sin\pi\omega_{21}}{\sin\pi\omega_2 \sin\pi\omega_{31}} - e^{-i\pi(\omega_{12}+\omega_{32})} \right) \frac{V_2 V_2}{\sin\pi\omega_{21} \sin\pi\omega_{23}} \left. \right] \\
& - \frac{2s}{t_1 t_2 t_3} (|s_1|)^{\omega_1} (|s_3|)^{\omega_3} \int \frac{d\omega'_2}{2\pi i} (e^{-i\pi|s_2|})^{\omega'_2} \left(\frac{e^{-i\pi\omega_{31}}}{\sin\pi\omega_{13}} + \frac{e^{-i\pi\omega_{13}}}{\sin\pi\omega_{31}} \right) (V_{\text{cut}} - V_p).
\end{aligned}$$

It is important to study the infrared singularities of the phases of this expression. First we note that the prefactor $e^{-i\pi\omega_2}$ contains, in lowest order in a , the $1/\epsilon$ singularity of the gluon trajectory (44). All other phase factors contain differences of trajectory functions and are finite as $\epsilon \rightarrow 0$. Expanding the square brackets in powers of a we arrive at (107):

$$\frac{A_{2 \rightarrow 4}}{\Gamma(t_1)\Gamma(t_3)} = \frac{2s}{t_1 t_2 t_3} g^2 C(q_2, q_1) C(q_3, q_2) (|s_1|)^{\omega_1} (|s_3|)^{\omega_3}.$$

$$\begin{aligned}
& e^{-i\pi\omega_2} (|s_2|)^{\omega_2} \left[1 + i \frac{\pi}{2} \left(\omega_1 + \omega_2 + a \left(\ln \frac{\kappa_{12}}{\mu^2} - \frac{1}{\epsilon} \right) + \omega_3 + \omega_2 + a \left(\ln \frac{\kappa_{23}}{\mu^2} - \frac{1}{\epsilon} \right) \right) \right] - 2i\pi \frac{2s}{t_1 t_2 t_3} \int \frac{d\omega'_2}{2\pi i} (e^{-i\pi|s_2|})^{\omega'_2} V_{\text{cut}}.
\end{aligned} \tag{E7}$$

Following the steps described in Sec. IV B we factor out the gluon trajectory (details are presented in [45]):

$$\int \frac{d\omega'_2}{2\pi i} (e^{-i\pi|s_2|})^{\omega'_2} V_{\text{cut}} = g^2 C(q_2, q_1) C(q_3, q_2) (e^{-i\pi|s_2|})^{\omega_2} \int \frac{d\omega'_2}{2\pi i} (e^{-i\pi|s_2|})^{\omega'_2} V_{\text{cut, reduced}}. \tag{E8}$$

Insertion into (E7) leads:

$$\begin{aligned}
& \frac{A_{2 \rightarrow 4}}{\Gamma(t_1)\Gamma(t_3)} = \frac{2s}{t_1 t_2 t_3} (|s_1|)^{\omega_1} (|s_3|)^{\omega_3} (|s_2|)^{\omega_2} g^2 C(q_2, q_1) C(q_3, q_2) e^{-i\pi\omega_2} \\
& \left[1 + i \frac{\pi}{2} \left(\omega_1 + \omega_2 + a \left(\ln \frac{\kappa_{12}}{\mu^2} - \frac{1}{\epsilon} \right) + \omega_3 + \omega_2 + a \left(\ln \frac{\kappa_{23}}{\mu^2} - \frac{1}{\epsilon} \right) \right) - 2i\pi \int \frac{d\omega'_2}{2\pi i} (e^{-i\pi|s_2|})^{\omega'_2} V_{\text{cut, reduced}} \right].
\end{aligned} \tag{E9}$$

The one-loop approximation of the Regge cut contribution, (105), is infrared singular:

$$g^2 C(q_2, q_1) C(q_3, q_2) \int \frac{d\omega'_2}{2\pi i} (e^{-i\pi|s_2|})^{\omega'_2} V_{\text{cut, reduced}} = g^2 \frac{C(q_2, q_1) C(q_3, q_2)}{2} \left[a \left(\ln \frac{\kappa_{123} \mu^2}{q_1^2 q_2^2} + \frac{1}{\epsilon} \right) + \dots \right], \tag{E10}$$

whereas the two-loop and higher order terms of $V_{\text{cut, reduced}}$ can be shown to be infrared finite [45]. As a consequence, in (E9) the coefficient in the square brackets is infrared finite, and the singularities are collected in the overall phase factor $e^{-i\pi\omega_2}$.

For completeness we also list those energy discontinuities which do not vanish in this kinematic region, the discontinuity in the total energy s and the discontinuity in s_2 . We again start from the analytic representation (E2). After some algebra (which includes approximating phase factors by unity) we find⁴:

$$\text{disc}_s \frac{A_{2 \rightarrow 4, \text{cut}}}{\Gamma(t_1)\Gamma(t_3)} \approx \frac{-\pi s}{t_1 t_2 t_3} (|s_1|)^{\omega_1} \int \frac{d\omega'_2}{2\pi i} (|s_2|)^{\omega'_2} V_{\text{cut}} (|s_3|)^{\omega_3}. \tag{E11}$$

In a similar way we compute the discontinuity in s_2 :

⁴We use the definition $\text{disc} f(s) = \frac{1}{2i} (f(s+i\epsilon) - f(s-i\epsilon))$.

$$\text{disc}_{s_2} \frac{A_{2 \rightarrow 4, \text{cut}}}{\Gamma(t_1)\Gamma(t_3)} \approx \frac{-\pi s}{t_1 t_2 t_3} (|s_1|)^{\omega_1} \int \frac{d\omega'_2}{2\pi i} (|s_2|)^{\omega'_2} \tilde{V}_{\text{cut}} (|s_3|)^{\omega_3}, \tag{E12}$$

where, instead of (103),

$$\begin{aligned}
\tilde{V}_{\text{cut}} &= \frac{t_2 N_c}{8} g^4 \int \frac{d^2 k d^2 k'}{(2\pi)^6} \left[C(q_2, q_1) \right. \\
& \left. - \frac{q_1^2}{(k+q_1)^2} C(k+q_2, k+q_1) \right] \\
& \times G^{(8_A)}(k+q_2, -k; k'+q_2, -k'; \omega'_2) \\
& \times \left[C(q_3, q_2) - C(k'+q_3, k'+q_2) \frac{q_3^2}{(k'+q_3)^2} \right].
\end{aligned} \tag{E13}$$

In lowest order we have:

$$\tilde{V}_{\text{cut}}^{(0)} = g^2 \frac{C(q_2, q_1) C(q_3, q_2)}{2\omega'_2} a \left(\ln \frac{\kappa_{123} \mu^2}{\kappa_{12} \kappa_{23}} + \frac{1}{\epsilon} \right). \tag{E14}$$

A completely analogous discussion applies to the case $3 \rightarrow 3$ (Figs. 9 and 11) in the multi-Regge region (for a detailed discussion of the ‘‘analytic’’ representation see [44]). Our ansatz is

$$\begin{aligned} \frac{A_{3 \rightarrow 3}}{\Gamma(t_1)\Gamma(t_3)} = & \frac{2s}{t_1 t_2 t_3} \int \frac{d\omega'_2}{2\pi i} \left[\left(\frac{|s_1|}{\mu^2} \right)^{\omega_1 - \omega'_2} \left(\frac{|s_{02}|}{\mu^2} \right)^{\omega'_2 - \omega_3} \left(\frac{|s|}{\mu^2} \right)^{\omega_3} \xi_{12'} \xi_{2'3} \xi_3 \frac{U_1(t_1, t_2, t_3, \kappa_{12}, \kappa_{23}; \omega'_2)}{\sin \pi \omega_{12'} \sin \pi \omega_{2'3}} \right. \\ & + \left(\frac{|s_3|}{\mu^2} \right)^{\omega_3 - \omega'_2} \left(\frac{|s_2|}{\mu^2} \right)^{\omega'_2 - \omega_1} \left(\frac{|s|}{\mu^2} \right)^{\omega_1} \xi_{32'} \xi_{2'1} \xi_1 \frac{U_1(t_1, t_2, t_3, \kappa_{12}, \kappa_{23}; \omega'_2)}{\sin \pi \omega_{32'} \sin \pi \omega_{2'1}} \\ & + \left(\frac{|s_{02}|}{\mu^2} \right)^{\omega'_2 - \omega_3} \left(\frac{|s_{13}|}{\mu^2} \right)^{\omega'_2 - \omega_1} \left(\frac{|s|}{\mu^2} \right)^{\omega_1 + \omega_3 - \omega'_2} \xi_{2'1} \xi_{2'3} \xi_{(1+3)2'} \frac{U_3(t_1, t_2, t_3, \kappa_{12}, \kappa_{23}, \kappa_{123}; \omega'_2)}{\sin \pi \omega_{2'1} \sin \pi \omega_{2'3} \sin \pi (\omega_1 + \omega_3 - \omega_{2'})} \\ & + \left(\frac{|s_{02}|}{\mu^2} \right)^{\omega(t_1)} \left(\frac{|s_{13}|}{\mu^2} \right)^{\omega(t_3)} \left(\frac{|s_2|}{\mu^2} \right)^{\omega'_2 - \omega_1 - \omega_3} \xi_3 \xi_1 \xi_{2'/(1+3)} \frac{U_4(t_1, t_2, t_3, \kappa_{12}, \kappa_{23}, \kappa_{123}; \omega'_2)}{\sin \pi (\omega_{2'} - \omega_1 - \omega_3)} \\ & \left. + \left(\frac{|s_3|}{\mu^2} \right)^{\omega_3 - \omega'_2} \left(\frac{|s_1|}{\mu^2} \right)^{\omega_1 - \omega'_2} \left(\frac{|s|}{\mu^2} \right)^{\omega'_2} \xi_{32'} \xi_{12'} \xi_{2'} \frac{U_5(t_1, t_2, t_3, \kappa_{12}, \kappa_{23}; \omega'_2)}{\sin \pi \omega_{32'} \sin \pi \omega_{12'}} \right], \end{aligned} \quad (E15)$$

where

$$\begin{aligned} \xi_{i(j+k)} &= e^{-i\pi(\omega_i - (\omega_j + \omega_k))} + 1, \\ \xi_{(i+j)k} &= e^{-i\pi((\omega_i + \omega_j) - \omega_k)} + 1. \end{aligned} \quad (E16)$$

The pieces labeled by 1, 2, 5 are ‘‘normal’’ and contain only Regge poles. They coincide with those of the $2 \rightarrow 4$ amplitude:

$$U_i = W_i, \quad i = 1, 2, 5, \quad (E17)$$

and they fit into the factorization pattern, The terms 3 and 4 have the extra Regge cut piece shown in Fig. 12 (right figure), which is described in terms of the color octet BFKL equation. In analogy with (100) and (101) one finds:

$$\begin{aligned} U_3 &= \frac{\sin \pi \omega_1 \sin \pi \omega_3}{\sin \pi \omega'_2} V_2(t_1, t_2, \kappa_{12}) \\ &\times \frac{1}{\omega'_2 - \omega_2} V_1(t_2, t_3, \kappa_{23}) \\ &+ \sin \pi \omega_{2'1} \sin \pi \omega_{2'3} (U_{\text{cut}} - U_p), \end{aligned} \quad (E18)$$

$$\begin{aligned} U_4 &= \frac{1}{\sin \pi \omega'_2} V_2(t_1, t_2, \kappa_{12}) \frac{1}{\omega'_2 - \omega_2} V_1(t_2, t_3, \kappa_{23}) \\ &+ (U_{\text{cut}} - U_p). \end{aligned} \quad (E19)$$

$$\begin{aligned} \frac{A_{3 \rightarrow 3}}{\Gamma(t_1)\Gamma(t_3)} = & \frac{2s}{t_1 t_2 t_3} (|s_1|)^{\omega_1} (|s_3|)^{\omega_3} \cdot (|s_2|)^{\omega_2} \left[e^{-i\pi\omega_2} \left(\frac{V_1}{\sin \pi \omega_{12}} + e^{-i\pi\omega_{12}} \frac{V_2}{\sin \pi \omega_{21}} \right) \left(e^{-i\pi\omega_{32}} \frac{V_1}{\sin \pi \omega_{23}} + \frac{V_2}{\sin \pi \omega_{32}} \right) \right. \\ & \left. - 2i \frac{V_1 V_2}{\sin \pi \omega_2} \right] + \frac{2is}{t_1 t_2 t_3} (|s_1|)^{\omega_1} (|s_3|)^{\omega_3} \int \frac{d\omega'_2}{2\pi i} (e^{-i\pi|s_2|})^{\omega'_2} U_{\text{cut}}. \end{aligned} \quad (E22)$$

The last term can be written as

$$\int \frac{d\omega'_2}{2\pi i} (e^{-i\pi|s_2|})^{\omega'_2} U_{\text{cut}} = g^2 C(q_2, q_1) C(q_3, q_2) (e^{-i\pi|s_2|})^{\omega_2} \int \frac{d\omega'_2}{2\pi i} (e^{-i\pi|s_2|})^{\omega'_2} U_{\text{cut, reduced}}. \quad (E23)$$

It is important to note that the one-loop approximation, $U_{\text{cut}}^{(0)}$,

The cut piece has been given in (103) and (105):

$$\begin{aligned} U_{\text{cut}} &= \frac{t_2 N_c}{8} g^4 \int \frac{d^2 k d^2 k'}{(2\pi)^6} \frac{q_1^2}{(k - q_1)^2} \\ &\times C(q_2 - k, q_1 - k) G^{(8_A)}(k, q_2 - k; k', q_2 - k'; \omega'_2) \\ &\times C(k' - k_2, k') \frac{q_3^2}{(k' - k_2)^2}, \end{aligned} \quad (E20)$$

with the lowest order approximation

$$U_{\text{cut}}^{(0)} = \frac{g^2 C(q_2, q_1) C(q_3, q_2)}{2\omega'_2} a \ln \frac{\kappa_{12} \kappa_{23}}{(\vec{q}_1 + \vec{q}_3 - \vec{q}_2)^2 q_2^2}. \quad (E21)$$

It contains Regge cut singularities, and breaks the factorization. Note that, in contrast to the $2 \rightarrow 4$ case, the one-loop approximation of the Regge cut term, has no $1/\epsilon$ pole, i.e. it is infrared finite.

In analogy with the $2 \rightarrow 4$ case, these Regge cut pieces does not show up in the physical region where all energies are positive. It is, again, only in the other physical region $s, s_2 > 0, s_1, s_3, s_{13}, s_{02} < 0$ where these pieces become visible. Proceeding in the same fashion as before (E6) we find for this region:

$$g^2 C(q_2, q_1) C(q_3, q_2) \int \frac{d\omega'_2}{2\pi i} (e^{-i\pi|s_2|})^{\omega'_2} U_{\text{cut, reduced}} = g^2 \frac{C(q_2, q_1) C(q_3, q_2)}{2} \left[a \left(\ln \frac{\kappa_{12} \kappa_{23}}{(\tilde{q}_1 + \tilde{q}_3 - \tilde{q}_2)^2 q_2^2} \right) + \dots \right], \quad (\text{E24})$$

as well as the higher order terms are infrared finite. We therefore write $A_{3 \rightarrow 3}$ in the following form:

$$\frac{A_{3 \rightarrow 3}}{\Gamma(t_1)\Gamma(t_3)} = \frac{2s}{t_1 t_2 t_3} (|s_1|)^{\omega_1} (|s_2|)^{\omega_2} (|s_3|)^{\omega_3} g^2 C(q_2, q_1) C(q_3, q_2) \cdot \left[1 + i \frac{\pi}{2} \left(\omega_1 + a \left(\ln \frac{\kappa_{12}}{\mu^2} - \frac{1}{\epsilon} \right) + \omega_3 + a \left(\ln \frac{\kappa_{23}}{\mu^2} - \frac{1}{\epsilon} \right) \right) - 2i\pi \int \frac{d\omega'_2}{2\pi i} (e^{-i\pi|s_2|})^{\omega'_2} U_{\text{cut, reduced}} \right]. \quad (\text{E25})$$

On the right-hand side, the square bracket term is infrared finite. This shows that the infrared structure of $A_{3 \rightarrow 3}$ is quite different from $A_{2 \rightarrow 4}$.

We conclude this section by listing the discontinuities in the energies s and s_2 :

$$\text{disc}_s \frac{A_{3 \rightarrow 3, \text{cut}}}{\Gamma(t_1)\Gamma(t_3)} \approx \frac{-\pi s}{t_1 t_2 t_3} (|s_1|)^{\omega_1} \int \frac{d\omega'_2}{2\pi i} \times (|s_2|)^{\omega'_2} U_{\text{cut}} (|s_3|)^{\omega_3}. \quad (\text{E26})$$

In a similar way we compute the discontinuity in s_2 :

$$\text{disc}_{s_2} \frac{A_{3 \rightarrow 3, \text{cut}}}{\Gamma(t_1)\Gamma(t_3)} \approx \frac{-\pi s}{t_1 t_2 t_3} (|s_1|)^{\omega_1} \int \frac{d\omega'_2}{2\pi i} \times (|s_2|)^{\omega'_2} \tilde{U}_{\text{cut}} (|s_3|)^{\omega_3}, \quad (\text{E27})$$

where \tilde{U} is obtained from U in the same way as \tilde{V} was obtained from V .

In order to compare these results with the BDS formula, we divide the scattering amplitudes by their Born approximation. For example, we obtain $M_{2 \rightarrow 3}$ by dividing $A_{2 \rightarrow 3}$ by the Born approximation

$$\frac{2s}{t_1 t_2} g^2 \delta_{\lambda_A \lambda_{A'}} \delta_{\lambda_B \lambda_{B'}} g C(q_2, q_1)$$

and $M_{2 \rightarrow 4}$ by dividing $A_{2 \rightarrow 4}$ by

$$\frac{2s}{t_1 t_2 t_3} g^2 \delta_{\lambda_A \lambda_{A'}} \delta_{\lambda_B \lambda_{B'}} g^2 C(q_2, q_1) C(q_3, q_2).$$

-
- [1] L. N. Lipatov, Sov. J. Nucl. Phys. **23**, 338 (1976); V. S. Fadin, E. A. Kuraev, and L. N. Lipatov, Phys. Lett. B **60**, 50 (1975); E. A. Kuraev, L. N. Lipatov, and V. S. Fadin, Sov. Phys. JETP **44**, 443 (1976); **45**, 199 (1977); I. I. Balitsky and L. N. Lipatov, Sov. J. Nucl. Phys. **28**, 822 (1978).
- [2] V. S. Fadin, R. Fiore, and M. I. Kotsky, Phys. Lett. B **387**, 593 (1996).
- [3] A. V. Kotikov and L. N. Lipatov, Nucl. Phys. **B582**, 19 (2000).
- [4] L. N. Lipatov, Nucl. Phys. **B365**, 614 (1991).
- [5] L. N. Lipatov, Phys. Lett. B **309**, 394 (1993).
- [6] L. N. Lipatov, Sov. Phys. JETP **63**, 904 (1986).
- [7] J. Bartels, Nucl. Phys. **B175**, 365 (1980); J. Kwiecinski and M. Praszalowicz, Phys. Lett. B **94**, 413 (1980).
- [8] L. N. Lipatov, Phys. Lett. B **251**, 284 (1990).
- [9] L. N. Lipatov, Nucl. Phys. **B548**, 328 (1999).
- [10] L. N. Lipatov, Padova Report No. DFPD/93/TH/70 (unpublished).
- [11] L. N. Lipatov, JETP Lett. **59**, 596 (1994); L. D. Faddeev and G. P. Korchemsky, Phys. Lett. B **342**, 311 (1995).
- [12] V. S. Fadin and L. N. Lipatov, Phys. Lett. B **429**, 127 (1998); M. Ciafaloni and G. Camici, Phys. Lett. B **430**, 349 (1998).
- [13] A. V. Kotikov and L. N. Lipatov, Nucl. Phys. **B661**, 19 (2003).
- [14] J. R. Andersen and A. Sabio Vera, Nucl. Phys. **B699**, 90 (2004).
- [15] A. Sabio Vera, Nucl. Phys. **B746**, 1 (2006).
- [16] L. N. Lipatov, *Proceedings of Conference ICTP on Perspectives in Hadronic Physics, Trieste, Italy, 1997*.
- [17] J. A. Minahan and K. Zarembo, J. High Energy Phys. **03** (2003) 013.
- [18] N. Beisert and M. Staudacher, Nucl. Phys. **B670**, 439 (2003).
- [19] A. V. Kotikov, L. N. Lipatov, and V. N. Velizhanin, Phys. Lett. B **557**, 114 (2003).
- [20] A. V. Kotikov, L. N. Lipatov, A. I. Onishchenko, and V. N. Velizhanin, Phys. Lett. B **595**, 521 (2004); **632**, 754(E) (2006).
- [21] S. Moch, J. A. M. Vermaseren, and A. Vogt, Nucl. Phys. **B688**, 101 (2004).
- [22] B. Eden and M. Staudacher, J. Stat. Mech. **11** (2006) P014.
- [23] N. Beisert, B. Eden, and M. Staudacher, J. Stat. Mech. **01** (2007) P021.
- [24] J. M. Maldacena, Adv. Theor. Math. Phys. **2**, 231 (1998).
- [25] S. S. Gubser, I. R. Klebanov, and A. M. Polyakov, Phys. Lett. B **428**, 105 (1998).
- [26] E. Witten, Adv. Theor. Math. Phys. **2**, 253 (1998).
- [27] A. V. Kotikov, L. N. Lipatov, A. Rej, M. Staudacher, and V. N. Velizhanin, J. Stat. Mech. **10** (2007) P10003.
- [28] R. C. Brower, J. Polchinski, M. J. Strassler, and C. I. Tan, J. High Energy Phys. **12** (2007) 005.

- [29] L. N. Lipatov, Nucl. Phys. **B452**, 369 (1995); Phys. Rep. **286**, 131 (1997).
- [30] E. N. Antonov, L. N. Lipatov, E. A. Kuraev, and I. O. Cherednikov, Nucl. Phys. **B721**, 111 (2005).
- [31] Z. Bern, L. J. Dixon, and V. A. Smirnov, Phys. Rev. D **72**, 085001 (2005).
- [32] V. Del Duca, A. Frizzo, and F. Maltoni, Nucl. Phys. **B568**, 211 (2000).
- [33] L. N. Lipatov and V. S. Fadin, Sov. J. Nucl. Phys. **50**, 712 (1989); V. S. Fadin and L. N. Lipatov, Nucl. Phys. **B406**, 259 (1993); V. S. Fadin, M. I. Kotsky, and L. N. Lipatov, Phys. Lett. B **415**, 97 (1997).
- [34] V. S. Fadin and L. N. Lipatov, Nucl. Phys. **B477**, 767 (1996).
- [35] M. Drummond, G. P. Korchemsky, and E. Sokatchev, Nucl. Phys. **B795**, 385 (2008).
- [36] S. G. Naculich and H. J. Schnitzer, Nucl. Phys. **B794**, 189 (2008).
- [37] Z. Bern, M. Czakon, L. J. Dixon, D. A. Kosower, and V. A. Smirnov, Phys. Rev. D **75**, 085010 (2007).
- [38] V. S. Fadin and R. Fiore, Phys. Lett. B **661**, 139 (2008).
- [39] O. Steinmann, Helv. Phys. Acta **33**, 257, 349 (1960).
- [40] I. T. Drummond, P. V. Landshoff, and W. J. Zakrzewski, Nucl. Phys. **B11**, 383 (1969); J. H. Weis, Phys. Rev. D **4**, 1777 (1971).
- [41] R. C. Brower, C. E. DeTar, and J. H. Weis, Phys. Rep. **14**, 257 (1974).
- [42] A. R. White, Nucl. Phys. **B67**, 189 (1973).
- [43] J. Bartels, Nucl. Phys. **B151**, 293 (1979).
- [44] J. Bartels, Nucl. Phys. **B175**, 365 (1980).
- [45] J. Bartels, L. N. Lipatov, and A. Sabio-Vera, CERN Report No. CERN-PH-TH-2008-125, DESY Report No. DESY-08-073.
- [46] J. M. Drummond, J. Henn, G. P. Korchemsky, and E. Sokatchev, Phys. Lett. B **662**, 456(2008).
- [47] L. F. Alday and J. Maldacena, J. High Energy Phys. **11** (2007) 068.
- [48] Z. Bern, L. J. Dixon, and D. A. Kosower, Phys. Rev. D **72**, 045014 (2005).
- [49] J. M. Drummond, J. Henn, G. P. Korchemsky, and E. Sokatchev, arXiv:0807.1095.
- [50] A. Brandhuber, P. Heslop, and G. Travaglini, Phys. Rev. D **78**, 125005 (2008).
- [51] N. Berkovits and J. Maldacena, J. High Energy Phys. **09** (2008) 062.
- [52] L. N. Lipatov, arXiv:0902.1444.
- [53] N. Beisert, R. Ricci, A. A. Tseytlin, and M. Wolf, Phys. Rev. D **78**, 126004 (2008).
- [54] N. Gromov, V. Kazakov, and P. Vieira, arXiv:0901.3753.
- [55] N. Gromov, V. Kazakov, A. Kozak, and P. Vieira, arXiv:0902.4458.
- [56] G. P. Korchemsky and A. V. Radyushkin, Nucl. Phys. **B283**, 342 (1987).
- [57] S. Mandelstam, Nuovo Cimento **30**, 1148 (1963).
- [58] D. Amati, A. Stanghellini, and S. Fubini, Nuovo Cimento **26**, 896 (1962).
- [59] R. C. Brower, H. Nastase, H. J. Schnitzer, and C. I. Tan, Nucl. Phys. **B814**, 293 (2009).
- [60] R. C. Brower, H. Nastase, H. J. Schnitzer, and C. I. Tan, arXiv:0809.1632.
- [61] Z. Bern, L. J. Dixon, D. A. Kosower, R. Roiban, M. Spradin, C. Vergu, and A. Volovich, Phys. Rev. D **78**, 045007 (2008).
- [62] J. M. Drummond, J. Henn, G. P. Korchemsky, and E. Sokatchev, Nucl. Phys. **B815**, 142 (2009).
- [63] V. Del Duca, C. Duhr, and E. W. N. Glover, J. High Energy Phys. **12** (2008) 097.